KfK 4947
Oktober 1991

# Numerical Study for a 50 kA Current Lead for the NET Model Coil Test in TOSKA-Upgrade

G. Friesinger, R. Heller, H. Katheder, G. Zahn
Institut für Technische Physik
Projekt Kernfusion

Kernforschungszentrum Karlsruhe

KERNFORSCHUNGSZENTRUM KARLSRUHE

Institut für Technische Physik

Projekt Kernfusion

KfK 4947

# Numerical study for a 50 kA current lead for the NET model coil test in TOSKA-Upgrade

G. Friesinger, R. Heller, H. Katheder, G. Zahn

Kernforschungszentrum Karlsruhe GmbH, Karlsruhe

Kernforschungszentrum Karlsruhe GmbH
Postfach 3640, 7500 Karlsruhe 1

ISSN 0303-4003

## Abstract

Based on the design of the heat exchanger of the 23 kA current lead for the POLO model coil, a current lead whose conductor is made of phosphorous deoxidized copper has been optimized for a nominal current of 50 kA. The stand-by (zero current operation) losses have been calculated to be 52 % of the nominal ones. The transient behaviour of the lead in case of a coolant loss at 50 kA has been investigated as well as its behaviour at 70 kA for a short time of 30 s. The conclusion is that for the 70 kA case the temperature at the bottom end of the heat exchanger stays below 6 K if the heat capacity of the helium flow has been taken into account. The loss of helium mass flow and a consecutive dump of the coil with a time constant of 3 s results in a fast rise of the cold end temperature either by using the heat capacity of the stagnant helium or not.

These results led to the decision to study the behaviour of a current lead with a smaller conductor cross section as well as the effect of a longer part of the heat exchanger equipped with $Nb_3Sn$ superconductor. This piece looks like a special superconducting connector bar. The results for the current lead with twice the current density and half the length are that the mass flow rate at nominal current increases by two to three percents whereas the one at zero current decreases only by six percents. If adding the conducting part equipped with superconductors, the stand-by mass flow rate decreases to 27 % of the nominal flow rate. In addition, the loss of helium mass flow leads to no increase of the bottom end temperature.

# Numerische Studie einer 50 kA Stromzuführung für den NET Modellspulentest in TOSKA Upgrade

## Zusammenfassung

Basierend auf dem Wärmetauscherkonzept für die 23 kA Stromzuführung für die POLO Modellspule wurde eine Stromzuführung für einen Nominalstrom von 50 kA optimiert, die aus SF-Kupfer besteht. Die Leerlaufverluste (ohne Strom) berechneten sich zu 52 % bezogen auf die Verluste bei 50 kA. Das transiente Verhalten im Falle eines Kühlmittelverlustes sowohl bei 50 kA als auch das Verhalten bei 70 kA für eine Dauer von 30 s wurden untersucht. Es zeigt sich für den 70 kA Überlastfall, daß die Temperatur am unteren Ende unter 6 K bleibt, wenn man die Wärmekapazität des stagnierenden Heliums berücksichtigt. Im Fall des Kühlmittelverlusts und einer sich anschließenden Schnellentladung der Spule mit einer Entladezeitkonstanten von 3 s ergibt sich ein schneller Temperaturanstieg am unteren Ende des Wärmetauschers.

Diese Ergebnisse führten zur Entscheidung, eine Stromzuführung mit halbem Kupferquerschnitt zu untersuchen. Es zeigt sich aber, daß der Massenstrom im Leerlauffall nur marginal reduziert wird (6 %), während der beim Nominalstrom unwesentlich höher ist. Erst wenn man den Kupferleiter verlängert und $Nb_3Sn$ Supraleiter parallel anordnet, verringert sich der Massenstrom im Leerlauffall auf 27 % des Nominalwertes. Hinzu kommt, daß der Kühlmittelverlust nicht zu einem Anstieg der Temperatur am unteren Ende führt.

# Table of Contents

## List of Illustrations

## List of Tables

# 1. Introduction

The TOSKA Upgrade facility is foreseen for testing model coils wound of conductors proposed for the superconducting toroidal and poloidal field coils of the **N**ext **E**uropean **T**orus NET. The model coils are assembled as a solenoidal stack in TOSKA. The concept definition and present analysis of the NET model coils is described in [1].

For the different scenarios proposed for the test, five current leads are needed which should carry a nominal current of 50 kA to reach a maximum field at the conductor of the inner coils of the coil stack of about 13.5 T, whereas the outer coils have a field of 12.5 T. 50 kA is the maximum current the power supply can achieve. To reach the operational i.e. mechanical and/or electrical limits a current drive scenario is planned which allows a temporary increase of the current in one coil by decreasing the current in the others. The maximum current one can get is 70 kA within 30 seconds.

During normal operation only four current leads are needed whereas the fifth one works in stand-by operation (defined as zero current operation). Therefore one aim is to keep the refrigerator power for this purpose as small as possible.

Last the current lead should be able to discharge the coil in case of the loss of mass flow in the lead without generating too much heat at the connection to the superconducting bus i.e. at least the coil should not quench.

In the following report a current lead which is cooled with forced-flow helium is proposed which will be able to fulfill the boundary conditions mentioned. In addition it will serve as a prototype lead for the superconducting magnet system of NET.

## 2. Design principles of the current lead

The current lead for the NET solenoid test in TOSKA-Upgrade with a nominal current of 50 kA is of the forced-flow type and consists of three parts i.e

- **the heat exchanger:**
  it transfers the conduction and ohmic heat to the helium coolant at a temperature range from 4.5 to 290 K. The main parameters are the heat transfer area, the helium flow cross section, the cross section of the current carrying and heat conducting conductor, and the length of the heat exchanger,
- **the cold end and connection to the superconducting bus:**
  it has to guarantee that anly a negligible heat will enter the superconducting bus bar. It is covered by $Nb_3Sn$ wires and has the same geometry as the heat exchanger itself.
- **the warm end terminal:**
  it serves as the connection to the water cooled power cables of the power supply and has to provide a good heat transfer to the helium coolant as well. Otherwise the temperature difference between the copper conductor and the helium coolant will rise strongly resulting, especially at low currents resp. at stand-by condition, in a helium outlet temperature being much too low to be tolerated. The reason is that the low outlet temperature of the helium gas would lead to condensation resp. freezing of the water vapour part of the air air surrounding the connecting lines. This would reduce the break down voltage drastically. This has been shown by calculations e.g. for the 23 kA current lead of the POLO model coil or for the 10 kA current lead for the EURATOM LCT coil.

In the following the role of warm end will be discussed more in detail

The importance of the heat exchange between the copper and the helium at the warm end terminal will rise if the current rises. The reason is that the optimum length of the heat exchanger, L, its current carrying cross section, A, and the operating current ,I, are correlated by

$$\frac{L\,I}{A} = \text{const.}$$

They are only depending on the copper and the heat transfer properties. This relation has been evaluated by assuming

- an ideal heat transfer which is independent of the temperature,
- the validity of the Wiedemann-Franz law which combines the electrical resistivity and the thermal conductivity via the Lorentz number, and
- a temperature profile which depends only on the residual resistivity ratio, RRR, of the conductor.

A detailed discussion of the relation given above can be found in [2].

Looking in more detail, the relationship between L, A and I is more complicated and can't be calculated analytically anymore. But qualitatively the relation can be used for estimations.

Generally spoken the length decreases with increasing current. In parallel the cold end losses increase with decreasing length. This leads to the fact that at low (or no) currents the mass flow has to be relatively high because the heat loss at the cold end has to be minimized.

This results in a mass flow rate for the heat exchanger itself which is much too high. Therefore the outlet temperature of the helium at the upper end of the heat exchanger will be very low e.g. about 240 K. The helium will enter the warm end region very cold. If the heat exchange at the warm end is bad, the helium gas will be only slightly warmed up whereas the copper temperature will rise due to the ohmic power production in the warm end. In existing designs the helium leaves the heat exchanger through small holes and flows in a concentric hole through the warm end up to the outlet on the top. Not much heat transfer area is present and the heat exchange is of course very bad because the only way to increase it would be to increase the Reynolds number considerably.

The computer code CURLEAD [3] was used for optimization of the current lead i.e. the heat exchanger, the cold end and the warm end. This code allows the optimization of the heat exchanger and the cold and warm ends simultaneously.

The design of the current lead proposed for the NET model coil test in TOSKA Upgrade is as follows:

- **heat exchanger**
  The heat exchanger itself is of the POLO type except the fact that now the cooling disks will be made out of OFHC-copper (in the POLO case they are made of phosphorous deoxidized copper).
- **cold end**
  The cold end is equipped with the same cooling disks as the heat exchanger itself but has in parallel $Nb_3Sn$ wires which take the current if the temperature will be below 10 K i.e. no heat production below that level and are of infinite resistivity above 16 K i.e. full heat production above 16 K. In between a linear increase of the current in the copper part is assumed. Due to this, the cold end transfers the conduction heat conducted out of the heat exchanger to the helium and **not** to the cold end.
- **warm end**
  Because for a high current current lead a good heat exchange at the warm end will be of great importance the following solution has been proposed:
  1. The outer diameter of the warm end copper rod has been chosen to be equal to the outer diameter of the heat exchanger.
  2. The concentric hole in the warm end has been enlarged up to 50 mm to get a technically usable space for a stack of copper disks like the heat exchanger disks which will be brazed into this hole (like is has been done for the cooling disks itself). In the calculation the disks take only part to the heat transfer but not to the heat conduction and heat production.

  The penalty for this modification is a higher pressure drop.

All calculations have been done by taking into account the radial temperature dependence of the heat transfer using a so-called variable rib efficiency [4]. This effects mainly the heat loss at the cold end.

In the study the current density of the conductor was first set to the one used in the POLO current lead (in the following named as **case I**). The main parameters of that lead are given in Table 1.

| Parameter | Unit | Value |
|---|---|---|
| Nominal current | kA | 22 |
| Current region | kA | 0 - 30 |
| Overall length | m | 2.32 |
| Bottom temperature of conductor $T_{Cu,bottom}$ | K | 4.5 |
| Inlet temperature of helium $T_{He,bottom}$ | K | 4.5 |
| Top temperature of conductor $T_{Cu,top}$ | K | 293 |
| Outlet temperature of helium $T_{He,top}$ | K | variable |
| Inlet pressure of helium | bar | 4 |
| RRR of conductor | | 6 |
| Heat exchanger length $l_{hex}$ | m | 1.90 |
| Length of superconducting part $l_{cold,1}$ | m | 0.15 |
| Length of superconducting part $l_{cold,2}$ for length adjustment at different currents | m | 0.95 |
| Cross section of conductor $A_{Cu}$ | $cm^2$ | 38.5 |
| Cooled perimeter of heat exchanger $P_{cool}$ | m | 11.6 |
| Cross section of helium $A_{He}$ | $cm^2$ | 36.5 |
| Inner diameter of cooling disks | mm | 70 |
| Outer diameter of cooling disks | mm | 135.7 |
| Transversal distance of cooling disks | mm | 2 |
| Disk thickness | mm | 1 |
| Hole diameter in cooling disks | mm | 1.6 |
| Minimum hole distance in cooling disks | mm | 2.5 |
| RRR of cooling disks | | 6 |
| Rib efficiency of cooling disks | | function of temperature |

**Table 1. General input parameters for the calculations of the POLO current lead**

This results in an increase of the outer diameter of the conductor from 70 mm to 90 mm. The outer diameter of the cooling disks are the same as for POLO. Also the length of the superconducting cold end heat exchanger was fixed to $l_{cold}$ = 150 mm as in the POLO case (there named $l_{cold,1}$, see

Table 1). The length of the warm end, $l_{warm}$ was set to 250 mm. Then the length of the heat exchanger itself, $l_{hex}$ , was varied to find out the optimum length.

In a second step the current density of the lead was increased by (arbitrarily chosen) a factor of two. The lengths of the cold resp. warm ends were fixed to the same numbers as in case I, and the length of the heat exchanger was varied again (**case II**).

As a consequence of the results of the cases I and II, a third one has been defined. The conductor cross section was set as the one in case II ($j = 2j_{POLO}$) whereas the total length of the heat exchanger i.e. $l_{cold} + l_{hex}$ was adjusted thus to get the length of case I. This results in a considerably larger length of the superconducting cold end heat exchanger i.e. $l_{cold} = 550$ mm. The last parameter set is named **case III**.

Table 2 summarizes the main boundaries for the calculations whereas in Table 3 and Table 4 the geometrical numbers which enter into the calculations are given. The cooling perimeter, $P_{cool}$, has been calculated by computing the total surface area of the cooling ribs resp. of the main conductor and dividing it by the heat exchanger length. In Figure 1 a schematic of the current lead is shown.

| Parameter | Unit | Value | | |
|---|---|---|---|---|
| | | case I | case II | case III |
| Nominal current | kA | 50 | | |
| Current region | kA | 0 - 70 (for short times) | | |
| Overall length | m | 1.15 | 0.75 | 1.15 |
| Bottom temperature of conductor $T_{Cu,bottom}$ | K | 4.5 | | |
| Inlet temperature of helium $T_{He,bottom}$ | K | 4.5 | | |
| Top temperature of conductor $T_{Cu,top}$ | K | 293 | | |
| Outlet temperature of helium $T_{He,top}$ | K | variable | | |
| Inlet pressure of helium | bar | 4 | | |
| RRR of conductor | | 6 | | |

**Table 2. General input parameters for the current lead calculations**

| Parameter | Unit | Value | | |
|---|---|---|---|---|
| | | case I | case II | case III |
| Heat exchanger length $l_{hex}$ | m | 0.75 | 0.35 | 0.35 |
| Length of superconducting part $l_{cold}$ | m | 0.15 | 0.15 | 0.55 |
| Cross section of conductor $A_{Cu}$ | $cm^2$ | 64.2 | 32.1 | 32.1 |
| Cooled perimeter of heat exchanger $P_{cool}$ | m | 8.85 | | |
| Cross section of helium $A_{He}$ | $cm^2$ | 30.05 | | |
| Inner diameter of cooling disks | mm | 90 | | |
| Outer diameter of cooling disks | mm | 135.7 | | |
| Transversal distance of cooling disks | mm | 2 | | |
| Disk thickness | mm | 1 | | |
| Hole diameter in cooling disks | mm | 1.6 | | |
| Minimum hole distance in cooling disks | mm | 2.5 | | |
| RRR of cooling disks | | 50 | | |
| Rib efficiency of cooling disks | | function of temperature | | |

**Table 3. Input parameters of the heat exchanger including the cold end for the current lead calculations**

| Parameter | Unit | Value |
|---|---|---|
| Warm end (transition region) | | |
| Length | m | 0.03 resp. 0.01 |
| Cross section of conductor $A_{Cu}$ | $cm^2$ | 100 resp. 125 |
| Cooled perimeter of heat exchanger $P_{cool}$ | m | 0.10 resp. 0.157 |
| Cross section of helium $A_{He}$ | $cm^2$ | 2.01 resp. 19.6 |
| Rib efficiency in transition region | | 0.95 |
| Warm end (heat exchanger) | | |
| Length | m | 0.210 |
| Cross section of conductor $A_{Cu}$ | $cm^2$ | 125 |
| Cooled perimeter of heat exchanger $P_{cool}$ | m | 2.15 |
| Cross section of helium $A_{He}$ | $cm^2$ | 7.0 |
| Inner diameter of conductor | mm | 50 |
| Diameter of cooling disks | mm | 50 |
| Transversal distance of cooling disks | mm | 2 |
| Disk thickness | mm | 1 |
| Hole diameter in cooling disks | mm | 1.6 |
| Minimum hole distance in cooling disks | mm | 2.5 |
| RRR of cooling disks | | 50 |
| Rib efficiency of cooling disks | | function of temperature |

**Table 4. Input parameters of the warm end for the current lead calculations**

It is considered that the copper volume of the cooling disks does not enter into the energy balance i.e. they don't carry any current and don't conduct heat, except they contribute to the heat capacity in case of a transient behaviour. In the latter case the heat capacity of the helium (stagnant resp. flowing) is also taken into account.

In the following chapter the calculation results will be presented. It should be mentioned that the current lead proposed in this report is optimized for the TOSKA-Upgrade facility in the Institut für Technische Physik at KfK. But the adaption to NET operation conditions is easily possible.

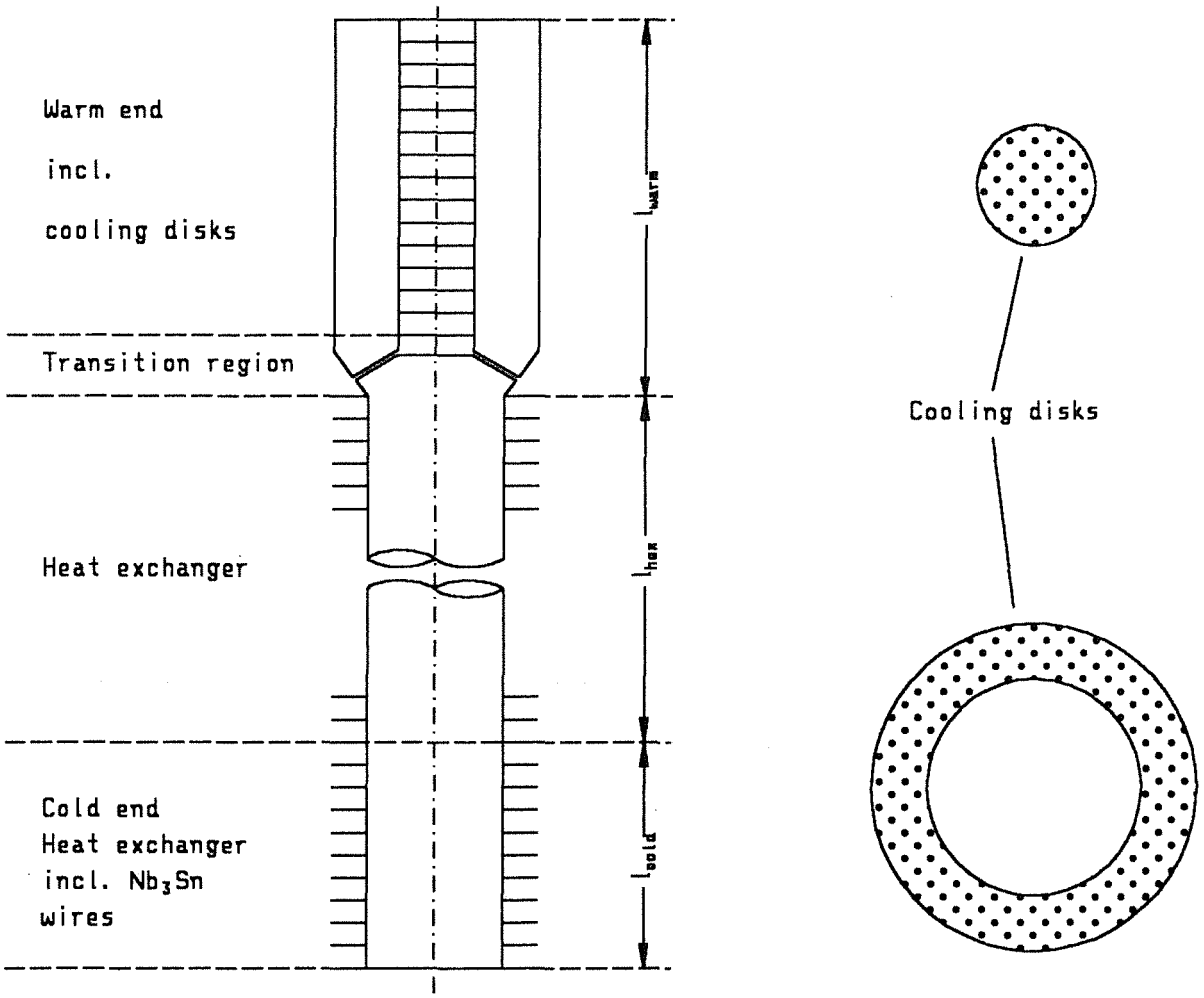


**Figure 1. Schematic of the current lead**

# 3. Results of calculations

## *3.1 Nominal operation*

First the current lead has been optimized with respect to its length and conductor cross section for the nominal current of 50 kA.

The optimizations for the cases I to III were done in the following way:

- The length of the heat exchanger $l_{hex}$ was first set to the value resulting from the simple relation of chapter 1.
  Then the mass flow rate was adjusted to fulfill two boundary conditions:
  1. To get a heat loss at the bottom end of less than the arbitrarily chosen value of 1 W. This can be done because for a forced-flow current lead the heat loss and the mass flow rate are decoupled, in contradiction to a bath cooled lead where the heat loss at the cold end produces the amount of mass flow for cooling the lead by evaporation of liquid helium.
  2. To get acceptable warm end losses.

The difference in length from that obtained by using the simple scaling law given in chapter 2. is about 10 cm (out of 75 cm).

The procedure described above was then repeated for different lengths of the heat exchanger i.e. $l_{hex}$.

In Figure 2 the helium mass flow rate is plotted versus the total length of the current lead for the cases I and II, i.e. for conductor cross sections of 64.2 $cm^2$ (full line) resp. 32.1 $cm^2$ (dashed line). For current leads which are too short, the bottom end heat losses determine the helium mass flow rate whereas for those which are too long the warm end heat losses dominate.

The minimum mass flow rates obtained for the optimum lengths of the cases I and II also vary slightly for the different cross sections i.e. different lengths, but only about 2 - 3 percents.

This is also true for the static losses (zero current) as will be shown in the next chapter.

The sensisitivity of the bottom end heat losses on the helium mass flow rate is shown in Figure 3. The full line belongs to case I, the dashed line to case II, and the dash-dotted line to case II.

The conclusion is that the current lead with the higher current density is more sensitive to changes of mass flow rates with respect to cold end losses than the one of case I. The effect is much more obvious if the length of the "superconducting" conductor part is drastically enlarged.

The temperature profiles of the optimized current leads are shown in Figure 4 whereas the numbers are summarized in Table 5 at the end of chapter 3.3.

The calculated helium mass flow rate of 2.7 g/s resp. 2.77 g/s can be converted to a specific loss of

$$\dot{q} = \frac{\dot{m}\,\Delta H}{I}$$

where

$\Delta H$ = heat of evaporation at 4.2 K, 1 bar = 20.9 J/g,

$\dot{m}$ = mass flow rate,

I = current.

In the case of the low current density current lead the result is $\dot{q}$ = 1.13 W/kA whereas for cases II and III the result is 1.16 W/kA. (This number serves only as a comparison with bath cooled leads).

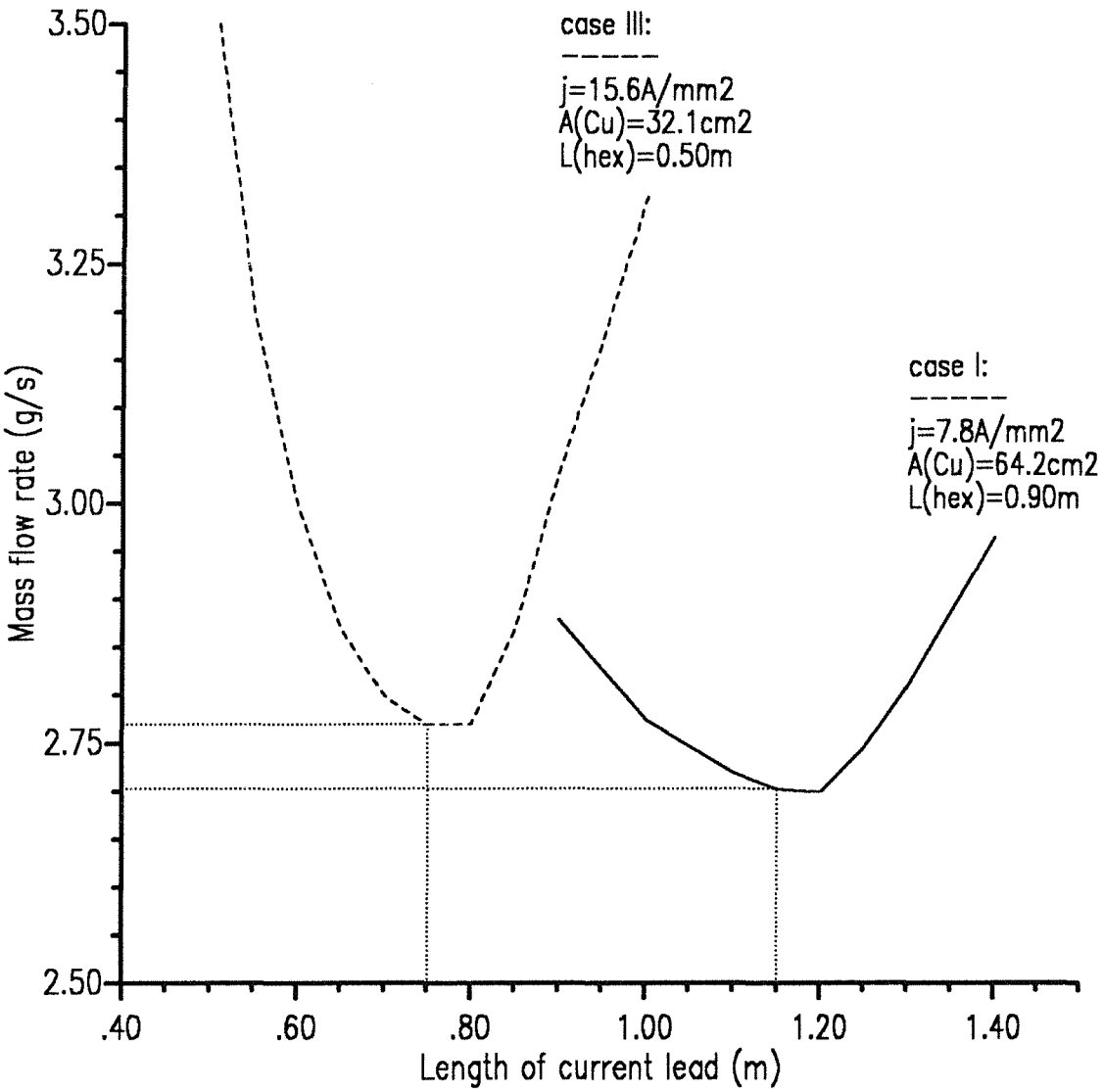


**Figure 2. Helium mass flow rate as a function of the current lead length for a current of 50 kA:** The full line belongs to case I, and the dashed line to case II

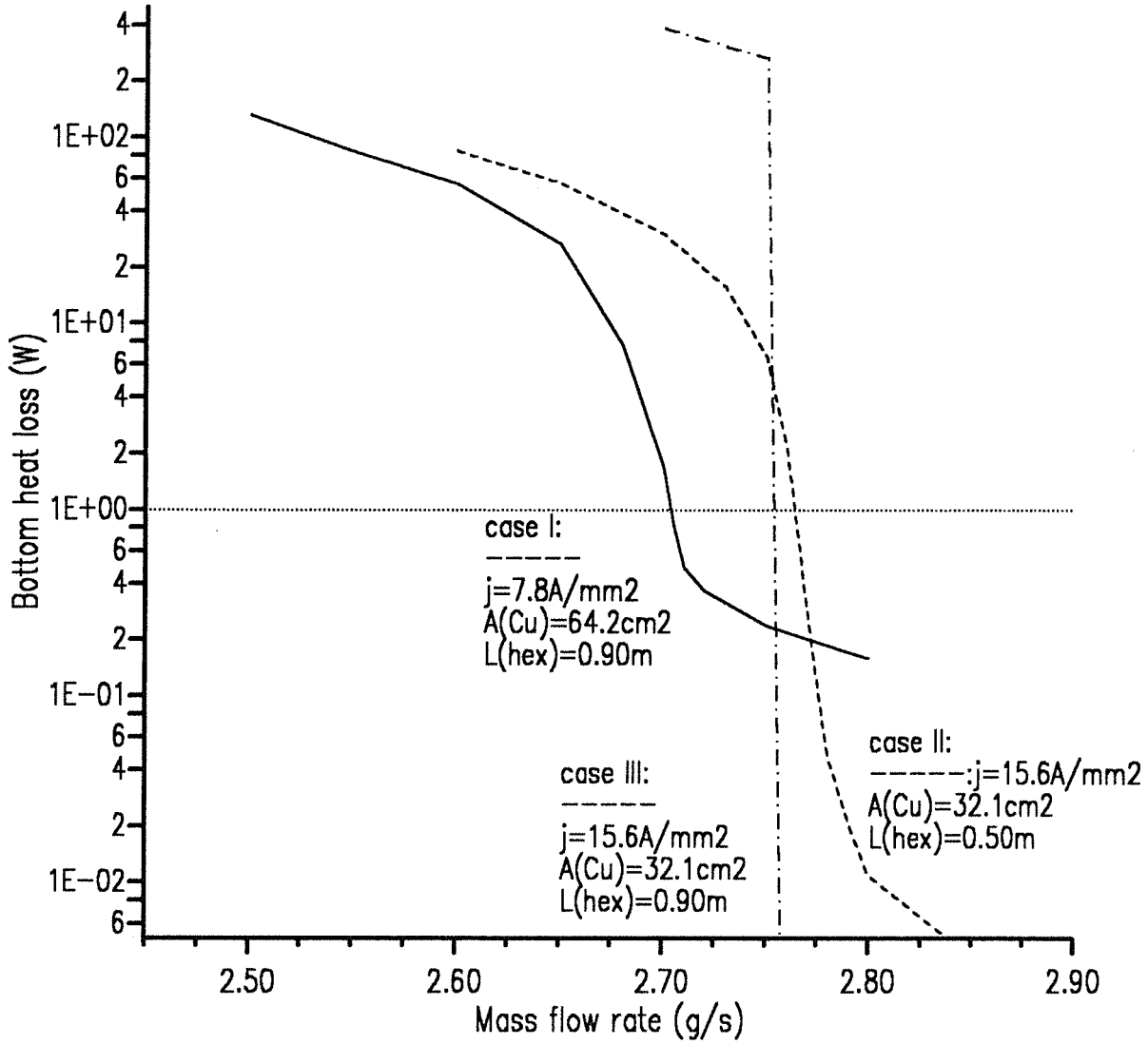


**Figure 3. Bottom heat loss as a function of the helium mass flow rate for a given length and a current of 50 kA:** The full line belongs to case I, the dashed line to case II and the dash dotted line to case III.

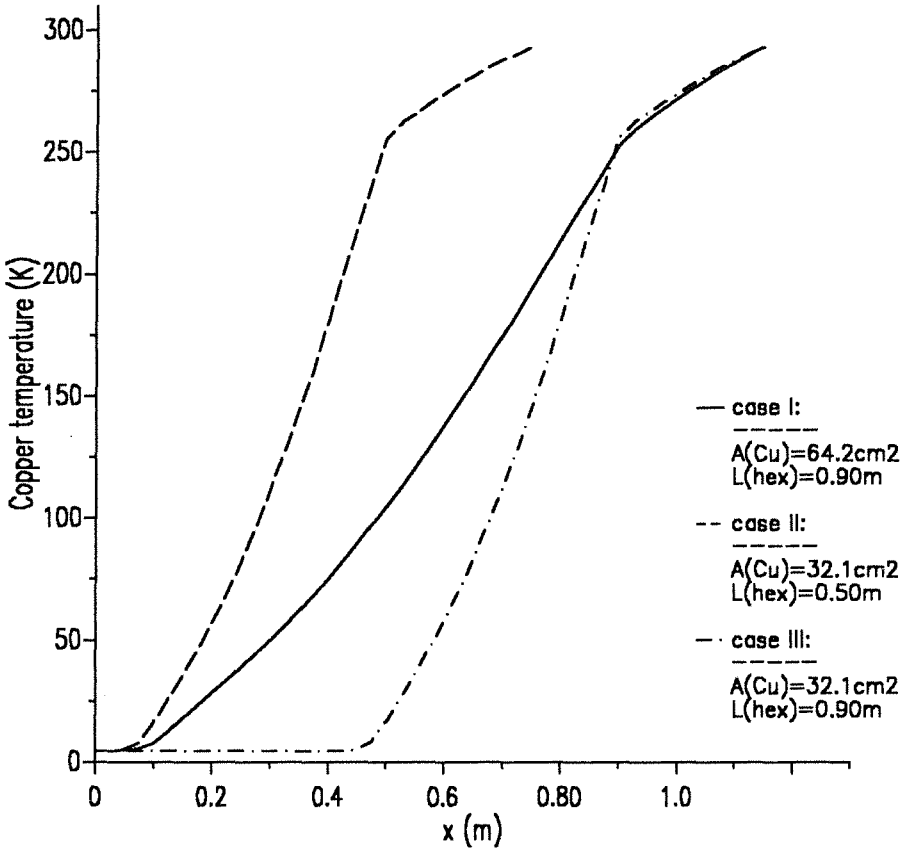


**Figure 4. Temperature distributions of the current leads at 50 kA:** The full line belongs to case I, the dashed line to case II and the dash dotted line to case III.

## 3.2 *Stand-by operation*

The temperature distributions for zero current have been calculated, too. The aim is to have a helium consumption as small as possible without getting heat out of the cold end.

Due to the fact that the high current carrying current lead has a short length and a big conductor cross section the losses for zero current are expected to be quite high.

The mass flow rate was adjusted also in the stand-by condition in order to get heat losses at the cold end of less than 1 W. This results in the temperature distributions shown in Figure 5. The corresponding numbers are given in Table 5. The mass flow rate for case I is 1.4 g/s which is about 50 % of the nominal mass flow rate. For case II the corresponding number is 1.3 g/s.

For case III the stand-by mass flow rate comes out to be 0.75 g/s i.e. only 27 % of the nominal one. The reason is the the longer length of the lead i.e. the increase of the superconducting part of the heat exchanger by 400 mm.

In Figure 6 the temperature difference between the conductor and the helium is plotted for zero current with (dashed line) and without (full line) the heat exchanger disks in the warm end for case I The effect of the enlarged cooling perimeter is clearly seen. The big temperature difference which arises within the (bad cooled) transition region between the heat exchanger and the warm end is reduced by the high cooling perimeter of the cooling disks. In the other case where only a small concentric slot has been cut into the warm end conductor the temperature difference will further increase leading to a helium outlet temperature of roughly 240 K. This is only a little higher than the end temperature of the heat exchanger where a good heat transfer exists.

The temperature difference between the conductor and the helium is shown for the nominal current of 50 kA as a dotted line. Its shape is very similar to the zero current one.

It should be mentioned that the mass flow rate for the self cooling condition will be smaller because the heat loss have to be balanced.

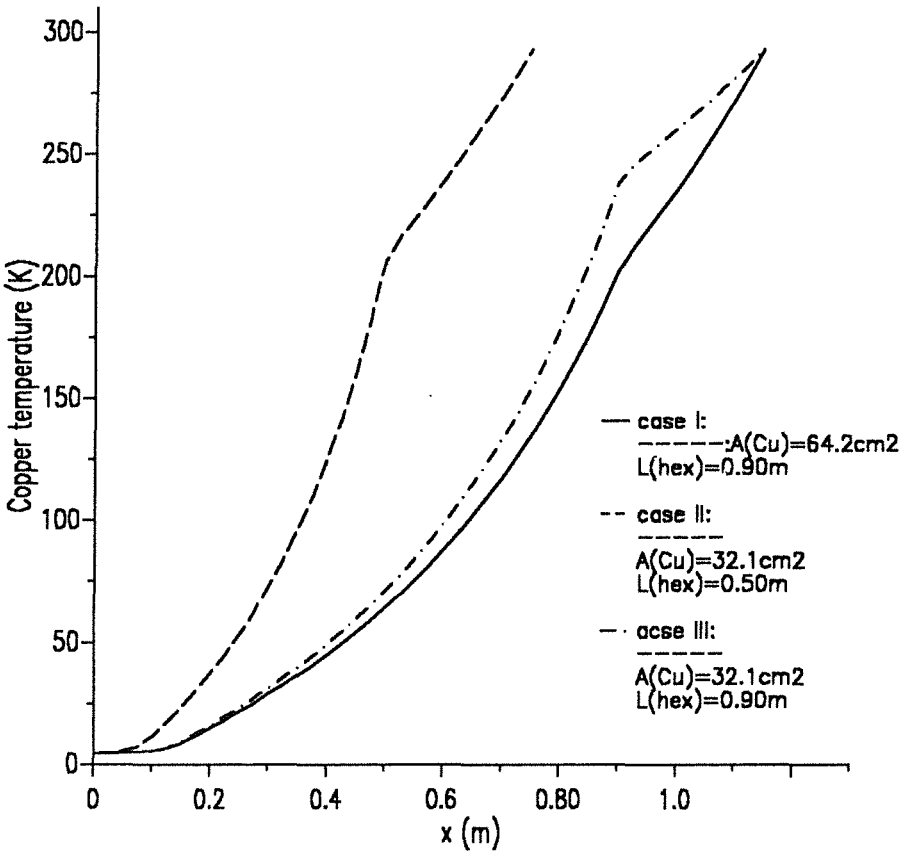


**Figure 5. Temperature distributions of the current leads for 0 kA:** The full line belongs to case I, the dashed line to case II and the dash dotted line to case III

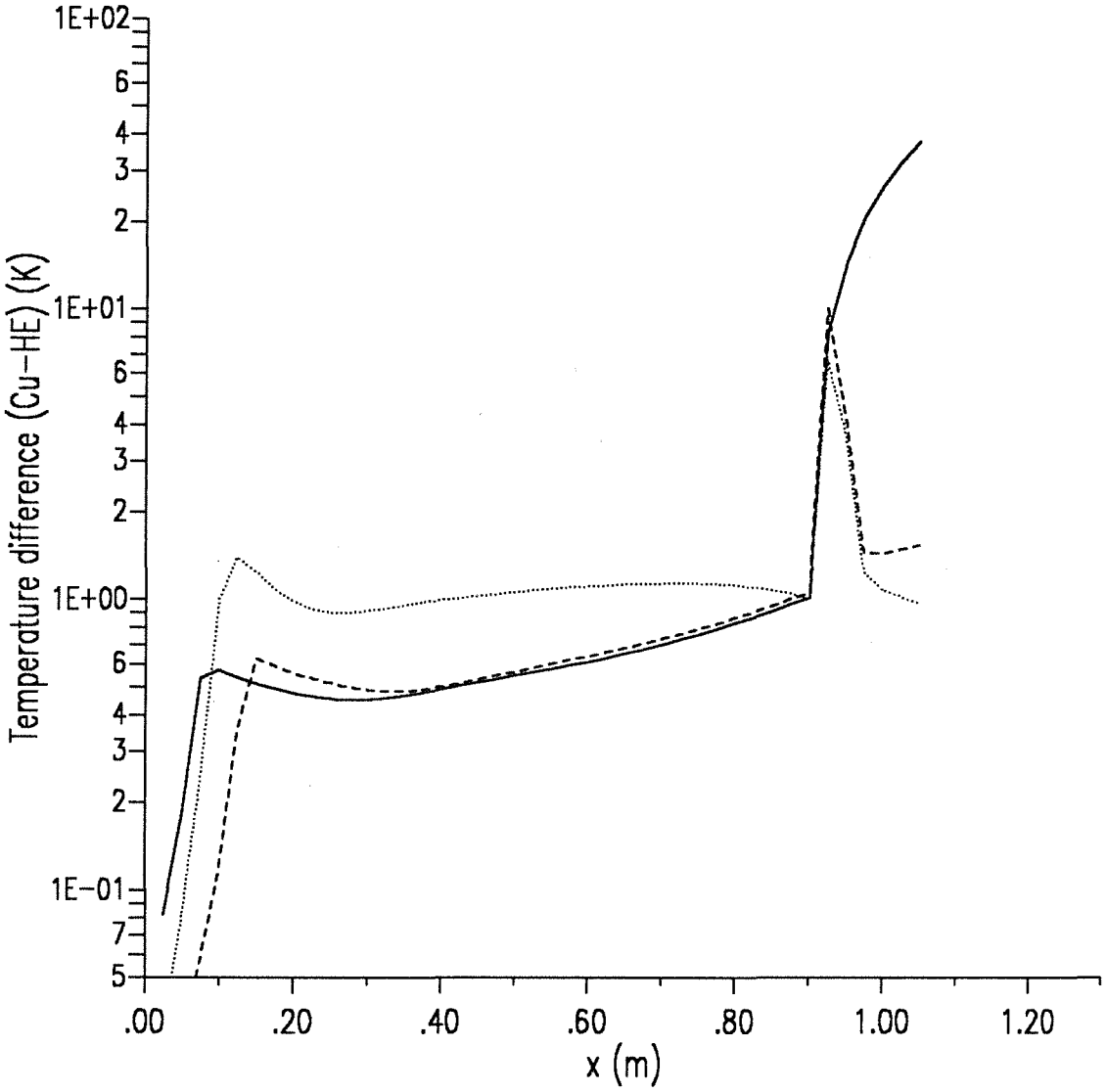


**Figure 6. Temperature difference between copper and helium vs length for case I:** The dashed line denotes the zero current case, the dotted line the 50 kA case where a good heat transfer is considered in the warm end. The full line corresponds to the zero current case without good heat transfer at the warm end.

## 3.3 *Steady-state load line of the current lead*

The load line of the current lead was calculated by adjusting the mass flow rate for 0 to 80 kA in steps of 10 kA thus to get minimum losses at the cold end and no overheating at the warm end. This has been done for cases I and III.

**It should be repeated here that for currents below the nominal one the mass flow rates are dominated by the cold end losses whereas for currents above it they are dominated by the warm end losses.**

Figure 7 shows the temperature distributions obtained for case I whereas in Figure 8 the temperature distributions of case III are shown. For the latter one the effect of the long supercondcuting part of the heat exchanger is clearly seen.

In Figure 9 the mass flow rate is plotted vs the current i.e. the load line of the current lead. This has been done for case I (full line) and case III dash dotted line) whereas for case II (full circles) only the numbers of 0 kA, 50 kA and 70 kA are shown. The reason is that the differences between the cases I and II are only marginal.

The rapid rise of the mass flow rate i.e. the helium consumption and finally the refrigerator power can be seen for currents above the nominal one. For example a 70 % higher mass flow is needed for 70 kA compared to 50 kA which is a 40 % increase in current but a factor of two in power. The numbers don't coincide because the temperature distributions (and therefore the resistances) of the lead are different for 50 and 70 kA.

The slope of the curves for case I and III are quite different: The current lead with the longer superconducitng part reaches the optimized curve at lower current and stays at this line up to the nominal current whereas in case I the optimized line is only touched exactly at the nominal current value for which the heat exchanger has been optimized.

The effect is not so clear if looking on the voltage drop dependence on the current. This can be seen in Figure 10. If looking on the results of case I (full line), it can be seen that the drastic increase at higher currents due to the increase of the resistance with temperature is partly cancelled by the reduction of resistance of the lead due to the higher mass flow needed to prevent overheating at the warm end. At lower currents (than the nominal one) the voltage drop-current dependence is rather linear.

The effect is different in case III (dash dotted line) because at lower currents the optimization criterion is not well defined i.e. the cold end losses are not very sensitive to the mass flow rate if a definite limit is reached, but the warm end losses are. For high currents the optimized mass flow rate is very accurate i.e. small changes of it lead to large changes in losses either at the cold or at the warm ends.

For case II only three numbers have been computed i.e. 0 kA, 50 kA, and 70 kA (full circles). They coincide with the numbers of case III.

The results of the load line calculations (case I and III) are summarized in Table 5

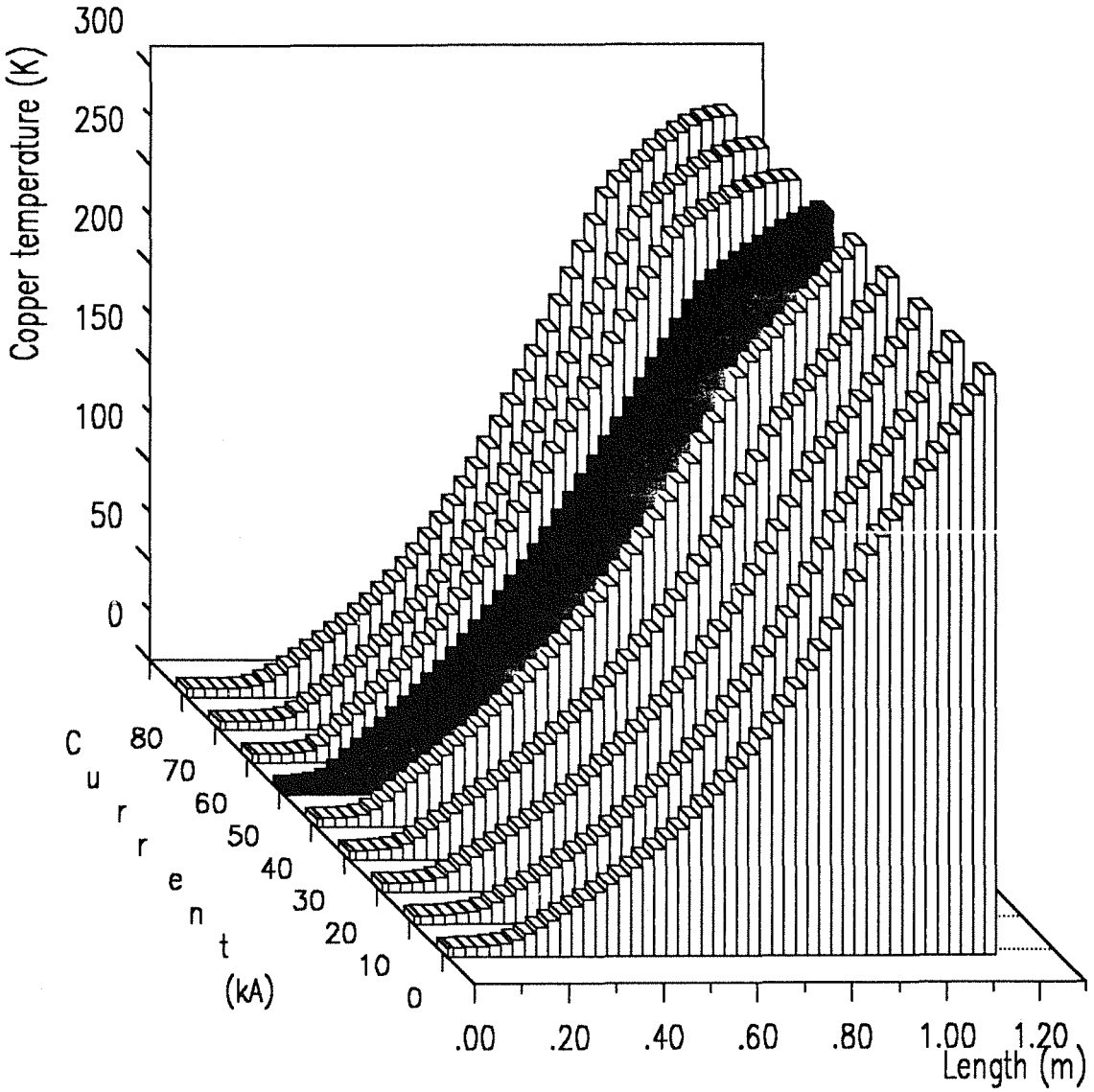


**Figure 7. Temperature distributions of the current lead for 0 to 80 kA (case I)**

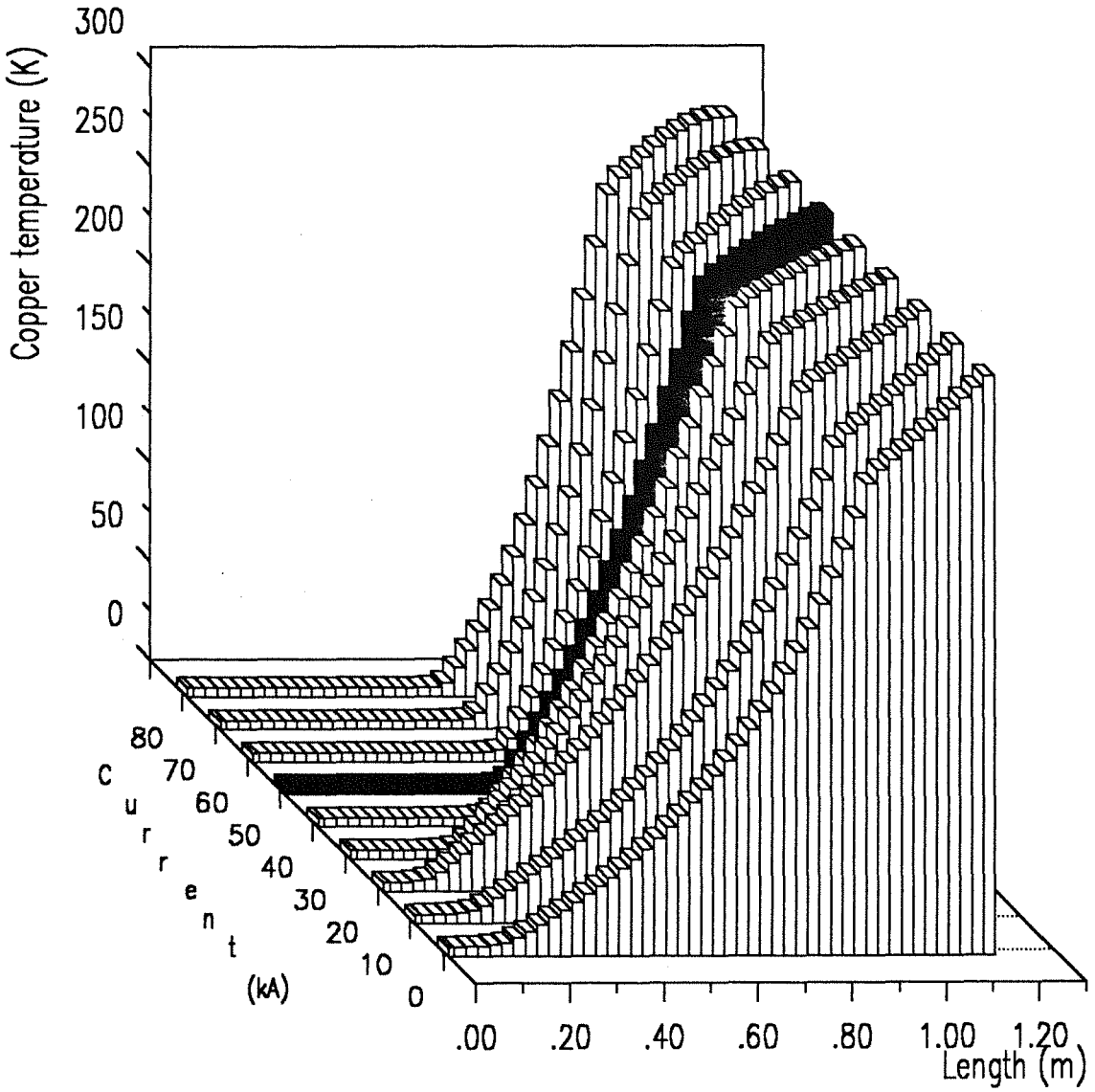


**Figure 8. Temperature distributions of the current lead for 0 to 80 kA (case III)**

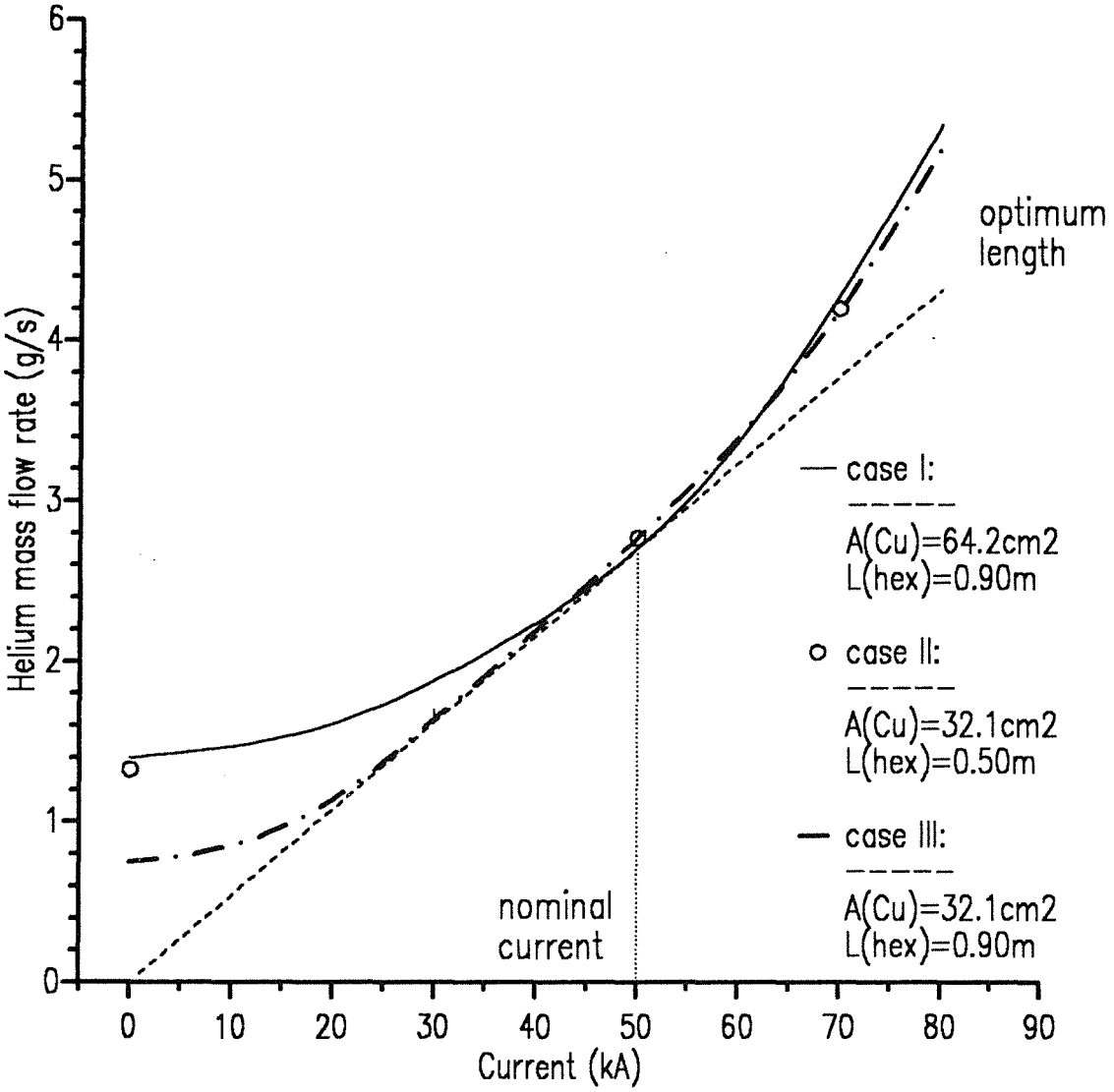


**Figure 9. Load line of the current lead for 0 to 80 kA:** The full line belongs to case I, the dash dotted line to case III whereas the full circles denote the numbers of case II

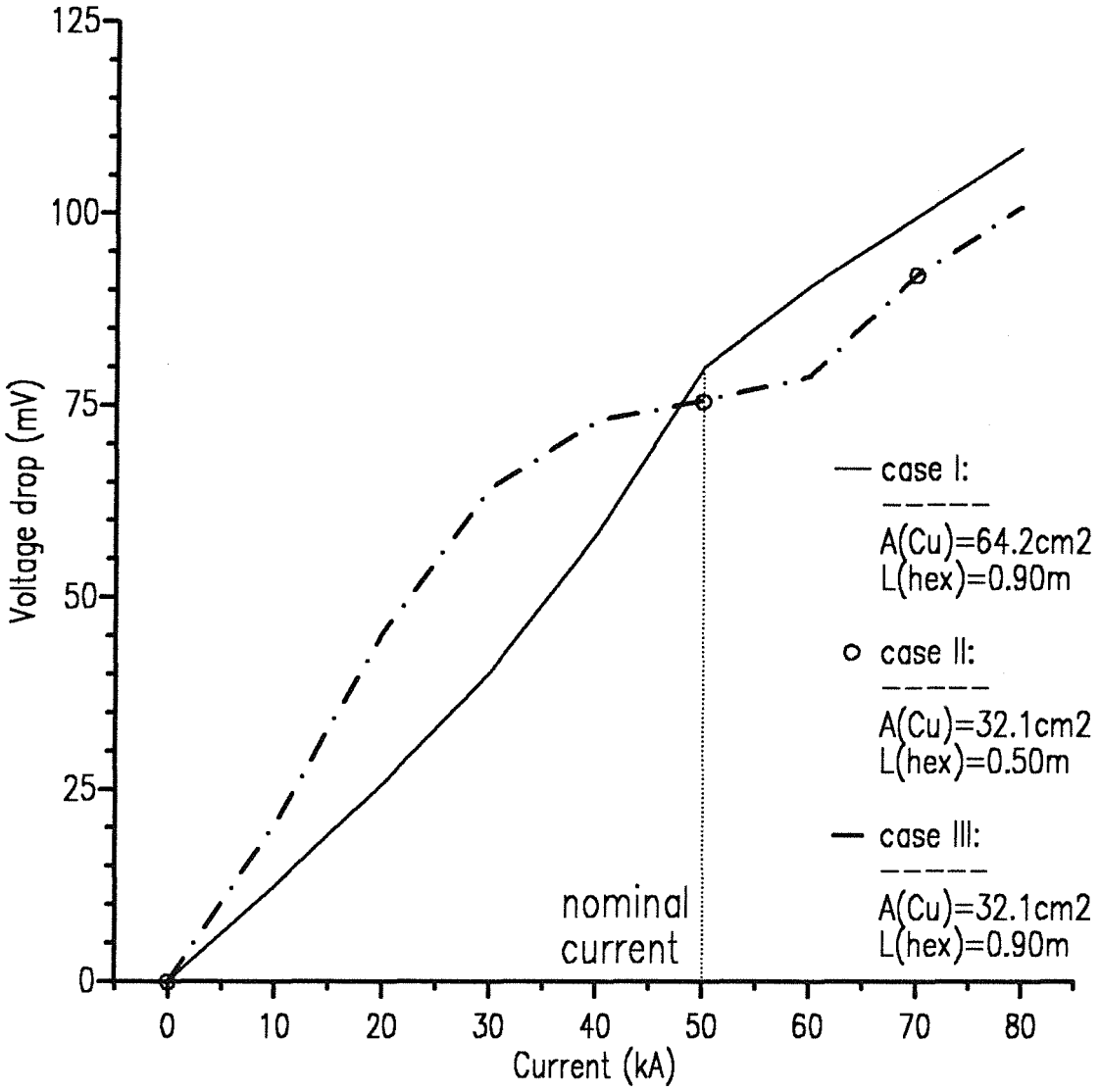


**Figure 10. Voltage drop vs current of the current lead for 0 to 80 kA:** The full line belongs to case I, the dash dotted line to case III whereas the full circles denote the numbers of case II

| I | $\dot{m}$ | ΔU | Δp | $Q_{bottom}$ | $T_{cold}$ | $T_{max,Cu}$ | $T_{top,He}$ |
|---|---|---|---|---|---|---|---|
| [kA] | $[\frac{g}{s}]$ | [mV] | [mbar] | [W] | [K] | [K] | [K] |
| case I | | | | | | | |
| 0 | 1.400 | 0.00 | 5.12 | 0.77 | 8.52 | 293.0 | 291.3 |
| 10 | 1.470 | 10.94 | 5.53 | 0.63 | 8.03 | 293.0 | 291.2 |
| 20 | 1.610 | 22.51 | 6.51 | 0.85 | 10.26 | 293.0 | 291.2 |
| 30 | 1.880 | 35.06 | 8.55 | 0.73 | 11.30 | 293.0 | 291.2 |
| 40 | 2.240 | 50.34 | 11.90 | 0.69 | 13.42 | 293.0 | 291.4 |
| 50 | 2.705 | 71.76 | 17.67 | 0.85 | 17.64 | 293.0 | 292.3 |
| 60 | 3.380 | 90.47 | 26.37 | 0.07 | 8.40 | 293.0 | 292.9 |
| 70 | 4.300 | 99.46 | 38.96 | 0.01 | 6.26 | 293.0 | 292.6 |
| 80 | 5.350 | 106.42 | 55.72 | 0.00 | 4.99 | 293.0 | 292.7 |
| case III | | | | | | | |
| 0 | 0.750 | 0.00 | 2.16 | 0.34 | 83.58 | 293.0 | 292.4 |
| 10 | 0.850 | 20.44 | 2.69 | 0.26 | 87.53 | 293.0 | 292.3 |
| 20 | 1.135 | 45.99 | 4.25 | 0.31 | 106.2 | 293.0 | 292.4 |
| 30 | 1.635 | 64.16 | 7.68 | 0.00 | 97.52 | 293.0 | 292.3 |
| 40 | 2.190 | 72.97 | 12.21 | 0.00 | 68.58 | 293.0 | 292.5 |
| 50 | 2.770 | 75.74 | 17.58 | 0.00 | 35.85 | 293.0 | 292.4 |
| 60 | 3.400 | 78.74 | 24.29 | 0.00 | 11.32 | 293.0 | 292.3 |
| 70 | 4.200 | 91.97 | 35.68 | 0.00 | 8.28 | 293.0 | 292.9 |
| 80 | 5.200 | 100.75 | 51.15 | 0.00 | 7.14 | 293.1 | 293.0 |

**Table 5. Main results of the load line calculations for cases I and III**

## 3.4 70 kA over-current for 30 seconds

During the test of the NET solenoid in the TOSKA Upgrade facility one current scenario to reach the mechanical limit and/or the critical current of the conductors is to increase the nominal current of 50 kA to 70 kA in one coil by discharging the others.

Therefore one has to know the behaviour of the current lead under a transient current load of 70 kA when starting from 50 kA.

Two cases have been studied. Starting from the 50 kA steady state distribution, the temperature distributions have been calculated for different times by using the Neumann condition at the cold end i.e. $Q_{cold,t} = Q_{cold,t=0s}$ varying the cold end temperature of the copper. The helium mass flow rate was set to the 50 kA case but

- case I:
  the heat capacity of the helium was not taken into account.
  the heat capacity of the helium was taken into account
- case III:
  the heat capacity of the helium was taken into account

The heat capacity of the heat exchanger disks has been used in all cases.

It should be mentioned that it is difficult to model the boundary condition at the cold end like in reality because neither the temperature (Dirichlet condition) nor the heat loss (Neumann condition) is fixed. On the other hand the Neumann condition seems to be more realistic because no helium bath will be available to fix the bottom end temperature for some time.

Figure 11 shows the copper temperature vs length for case I and no helium heat capacity is included. Figure 12 shows the same case but the helium heat capacity is now included. **The results are only different at lower lengths because here the heat capacity of the helium is much higher than that of the copper**. Figure 13 shows the results for case III where the helium heat capacity is also included.

Figure 14 shows the temperature of the conductor at the bottom end of the current lead as a function of the time for the different cases. The numbers are summarized in Table 6.

The general conclusion is that for an over-current of 70 kA within 30 s, the mass flow rate optimum for the 50 kA case is sufficient.

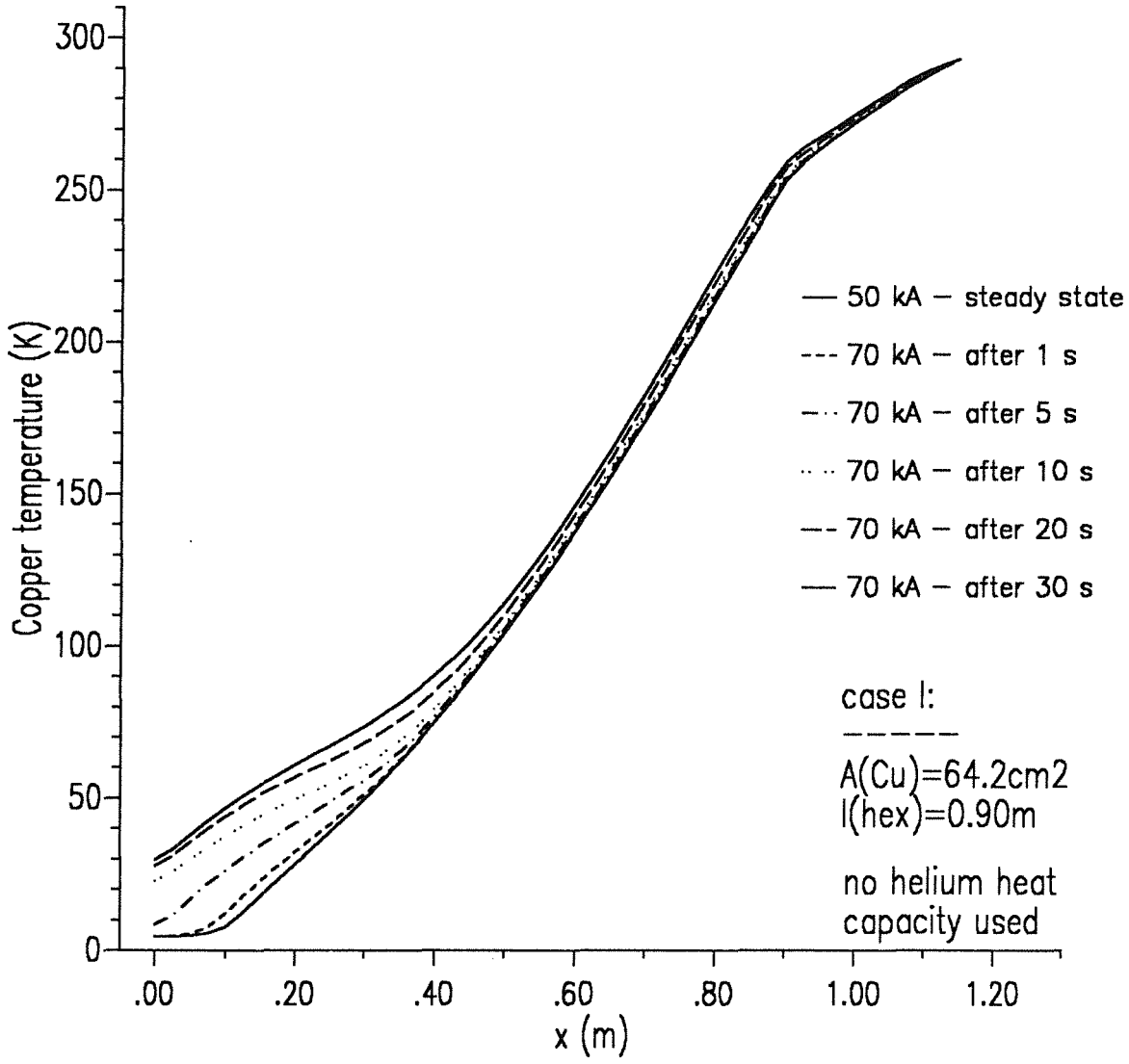


**Figure 11. Temperature distributions of the current lead in case of 70 kA over-current for 30 s (case I). The helium heat capacity has not been used:** The copper cross section is 64.2 cm², the heat exchanger length is 900 mm. The different lines correspond to different times

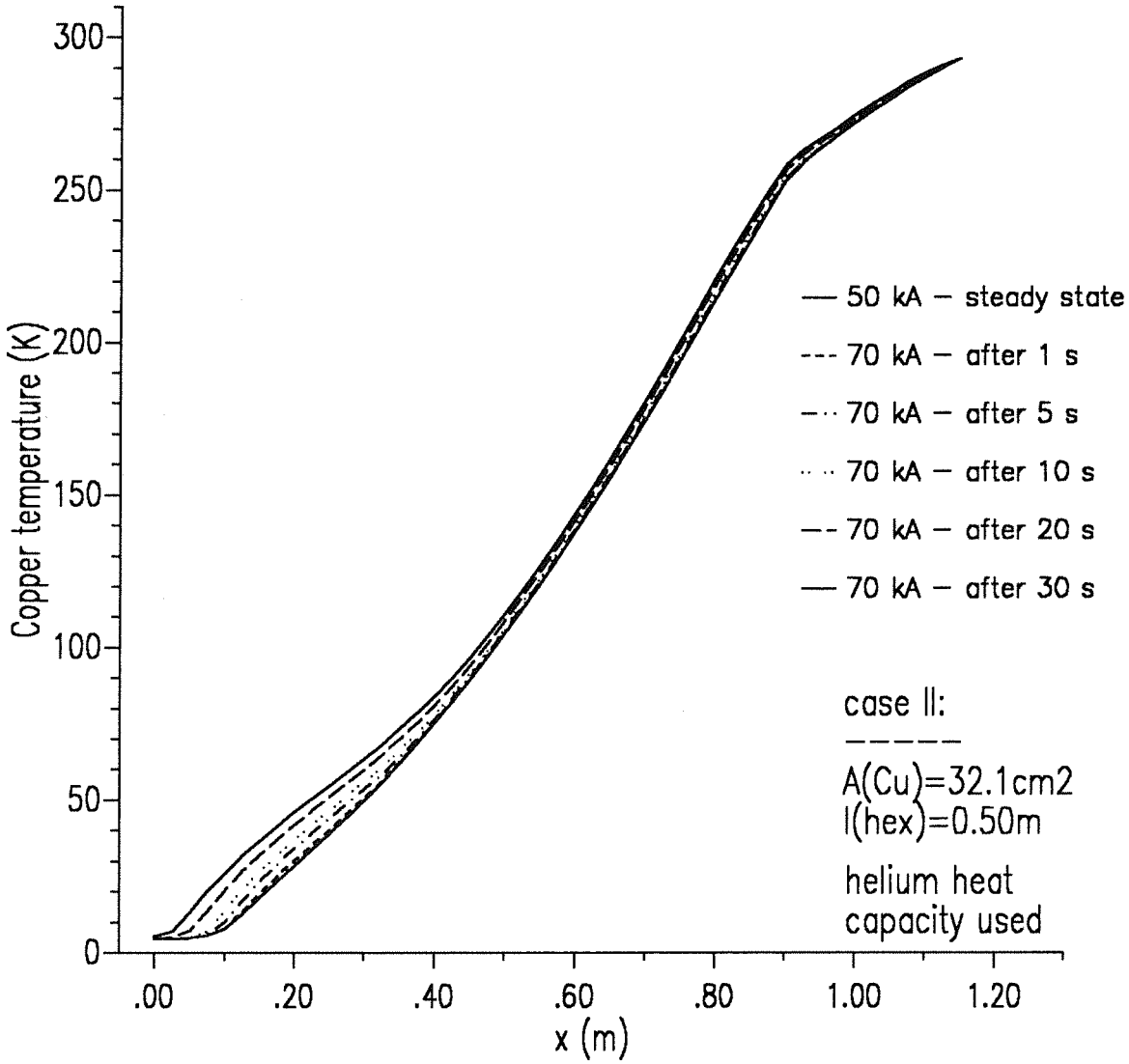


**Figure 12. Temperature distributions of the current lead in case of 70 kA over-current for 30 s. (case I). The helium heat capacity has been used:** The copper cross section is 32.2 cm², the heat exchanger length is 500 mm. The different lines correspond to different times

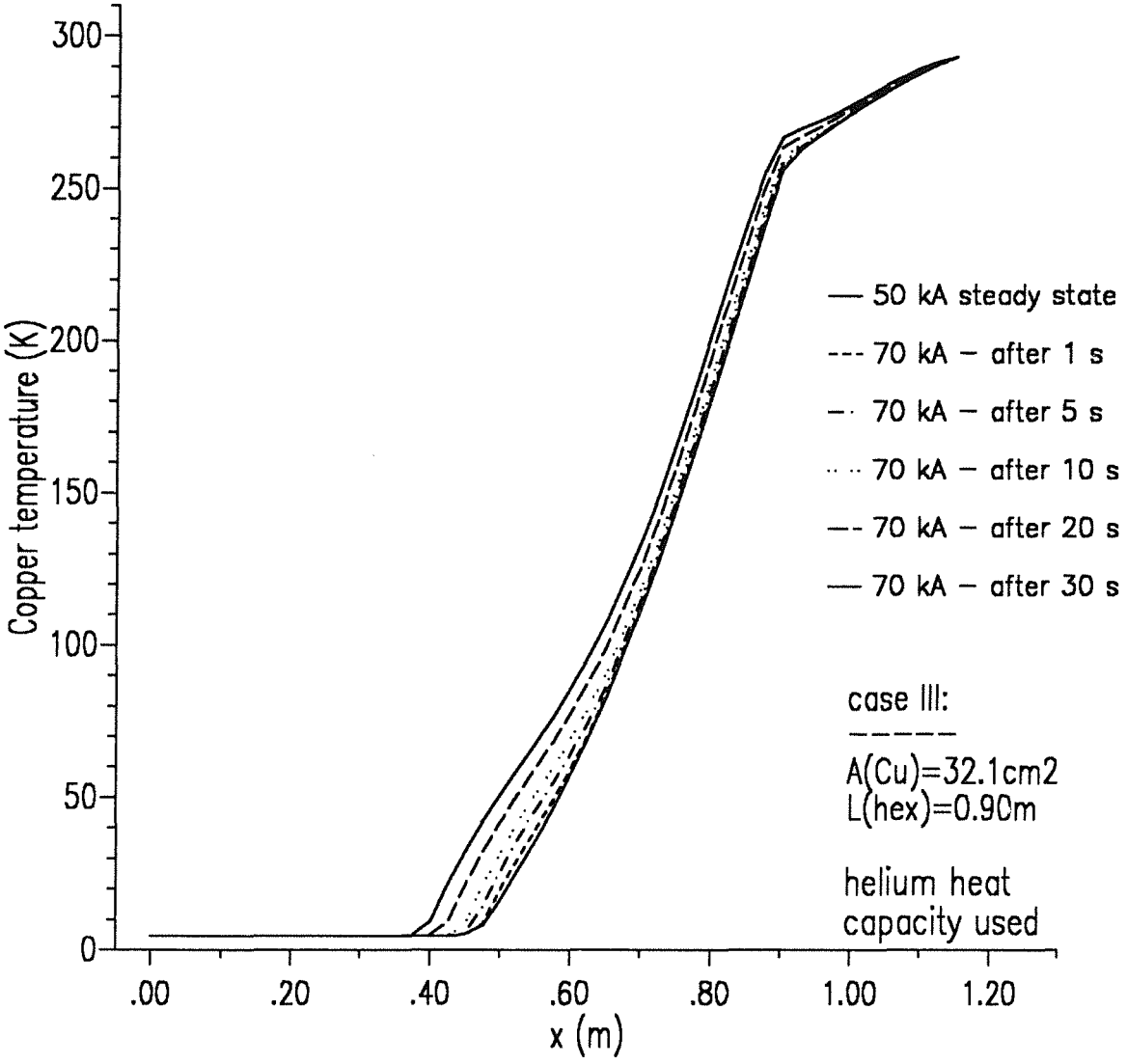


**Figure 13. Temperature distributions of the current lead in case of 70 kA over-current for 30 s. (case III). The helium heat capacity has been used:** The copper cross section is 32.1 cm², the heat exchanger length is 900 mm. The different lines correspond to different times

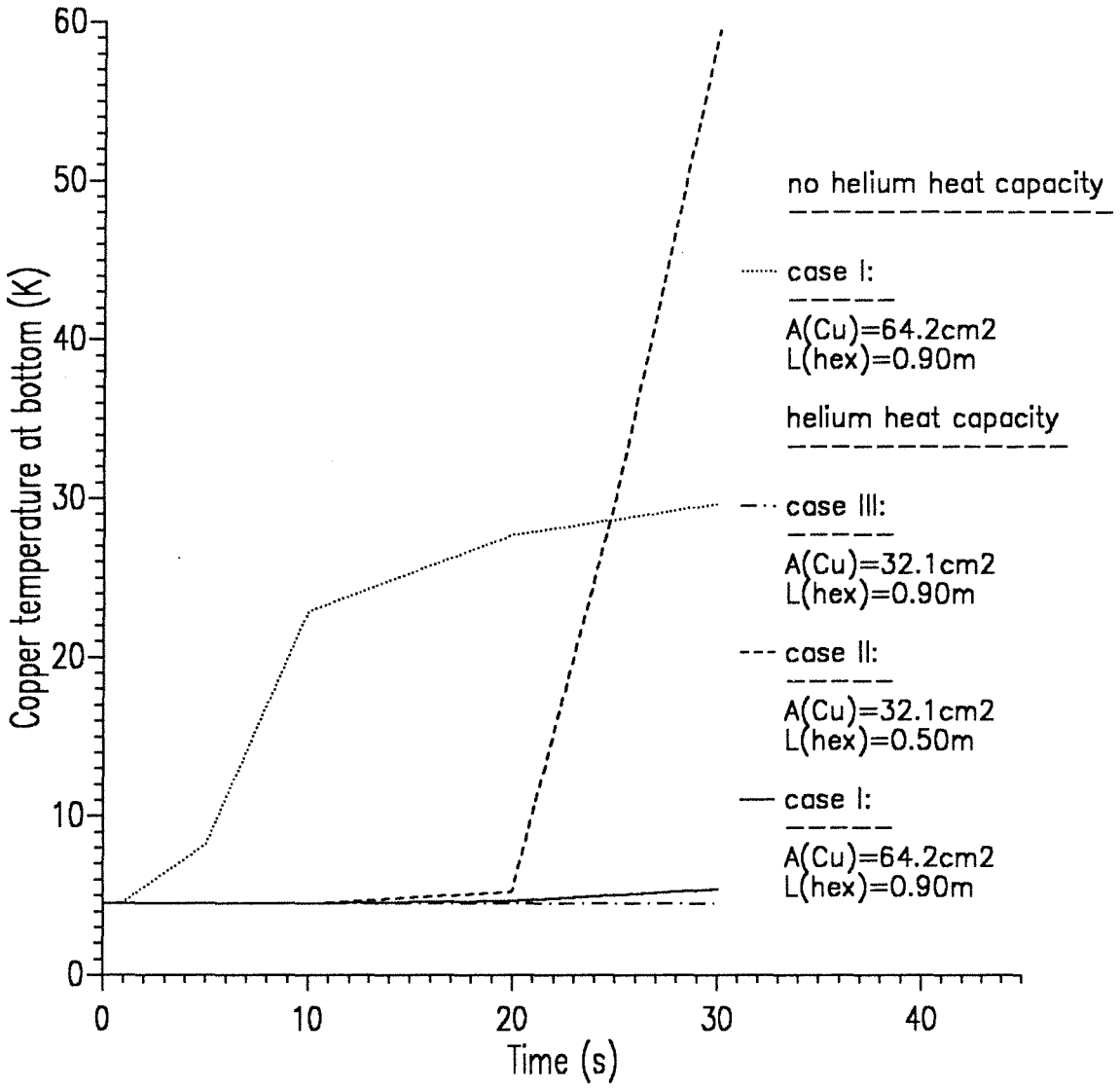


**Figure 14. Temperature of the conductor at the bottom end of the current lead vs time for 70 kA:** The dotted line corresponds to case I where the helium heat capacity has not been used, the full line to the same case but with the helium heat capacity inclueded, whereas the dashed and dash-dotted lines belong to cases II and III with the helium heat capacity included

| Time | $\dot{m}$ | ΔU | Δp | $T_{bottom}$ | $T_{cold}$ | $T_{max,Cu}$ | $T_{top,He}$ |
|---|---|---|---|---|---|---|---|
| [s] | $[\frac{g}{s}]$ | [mV] | [mbar] | [K] | [K] | [K] | [K] |
| case I<br>50 kA steady state | | | | | | | |
| 0 | 2.7 | 71.8 | 17.67 | 4.50 | 17.64 | 293.0 | 292.3 |
| 70 kA for 30 s (no He heat capacity considered) | | | | | | | |
| 1 | 2.7 | 101.6 | 17.64 | 4.63 | 22.8 | 293.0 | 292.3 |
| 5 | 2.7 | 105.3 | 17.74 | 8.26 | 34.3 | 293.0 | 292.3 |
| 10 | 2.7 | 107.8 | 17.85 | 22.93 | 44.0 | 293.0 | 292.4 |
| 20 | 2.7 | 110.3 | 18.00 | 27.72 | 50.9 | 293.0 | 292.5 |
| 30 | 2.7 | 112.5 | 18.14 | 29.70 | 54.2 | 293.0 | 292.6 |
| 70 kA for 30 s (He heat capacity included) | | | | | | | |
| 1 | 2.7 | 100.8 | 17.63 | 4.50 | 19.3 | 293.0 | 292.3 |
| 5 | 2.7 | 101.8 | 17.68 | 4.50 | 23.1 | 293.0 | 292.3 |
| 10 | 2.7 | 103.0 | 17.74 | 4.50 | 26.4 | 293.0 | 292.4 |
| 20 | 2.7 | 105.3 | 17.84 | 4.64 | 31.7 | 293.0 | 292.5 |
| 30 | 2.7 | 107.5 | 17.95 | 5.39 | 36.4 | 293.0 | 292.6 |
| case III<br>50 kA steady state | | | | | | | |
| 0 | 2.77 | 75.74 | 17.58 | 4.50 | 35.85 | 293.0 | 292.4 |
| 70 kA for 30 s (He heat capacity included) | | | | | | | |
| 1 | 2.77 | 106.83 | 17.60 | 4.50 | 39.37 | 293.0 | 292.43 |
| 5 | 2.77 | 109.46 | 17.67 | 4.50 | 45.70 | 293.0 | 292.48 |
| 10 | 2.77 | 112.52 | 17.74 | 4.50 | 50.85 | 293.0 | 292.52 |
| 20 | 2.77 | 118.76 | 17.91 | 4.50 | 59.58 | 293.0 | 292.59 |
| 30 | 2.77 | 125.27 | 18.07 | 4.50 | 67.61 | 293.0 | 292.64 |

**Table 6. Main results for 70 kA transient**

## 3.5 *Loss of helium coolant*

For safety reasons care has to be given to the emergency situation where a loss of helium mass flow through the current lead occurs while the mass flow through the coil will stay. The reason to assume a loss of helium mass flow through the current lead and at the same time a continuous flow through the coils is, that both supply circuits are separated. The cold circuit is driven by an independent pump whereas the lead circuit is connected directly to the refrigerator.

In the study two cases have been investigated. First the current lead is in a 50 kA steady state condition.

1. The mass flow rate will be stopped and the temperature distributions will be computed for 30 s while the current stays at nominal operation.
2. The mass flow rate will be stopped and the temperature distributions will be computed within 20 s while dumping the current with a dump time constant of $\tau = 3$ s.

The latter case has been calculated for the current lead case III, too.

In both cases the heat capacity of the stagnant helium has been included in the energy balance.

The boundary conditions at the cold end are the same as in the last section i.e. floating temperature of the conductor while the heat loss towards the superconducting bus is set to the initial value i.e. $Q_{cold,t} = Q_{cold,t=0s}$

Figure 15, Figure 17 and Figure 18show the temperature distributions for the three cases explained above whereas in Figure 16 the current decay versus time is plotted. The dashed line denotes the real current dump with a time constant of 3 s whereas the full step-like line is the approximation used in the calculations.

Figure 19 shows the bottom end temperature of the conductor of the current lead as a function of time. The difference for the two cases considered are not very big. The effect of the current dump is a lower temperature even with the inclusion of the heat capacity of the stagnant helium. Table 7 summarizes the numbers.

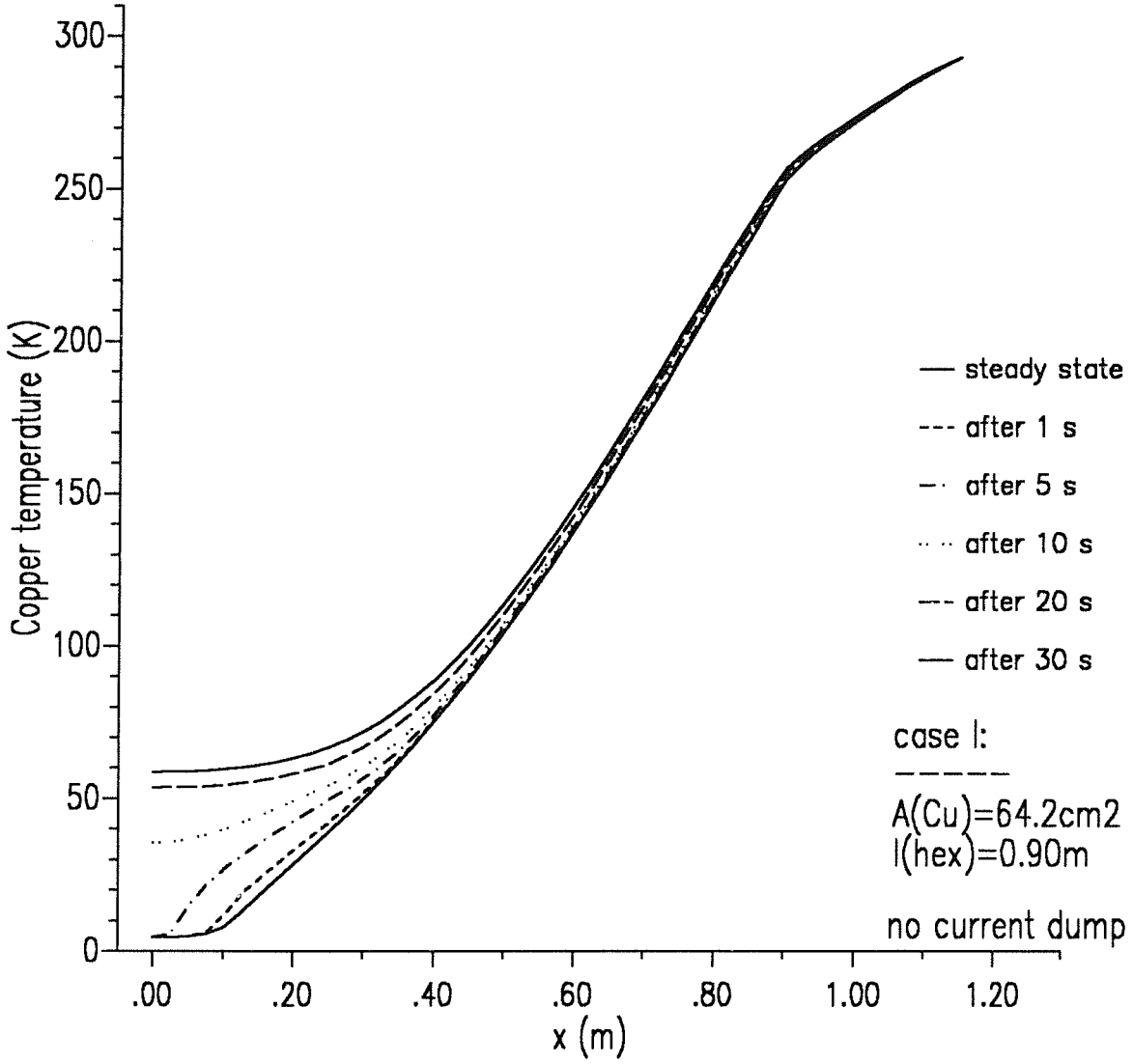


**Figure 15. Temperature distributions of the current lead in case of loss of mass flow and no current dump (case I):** The different lines correspond to different times

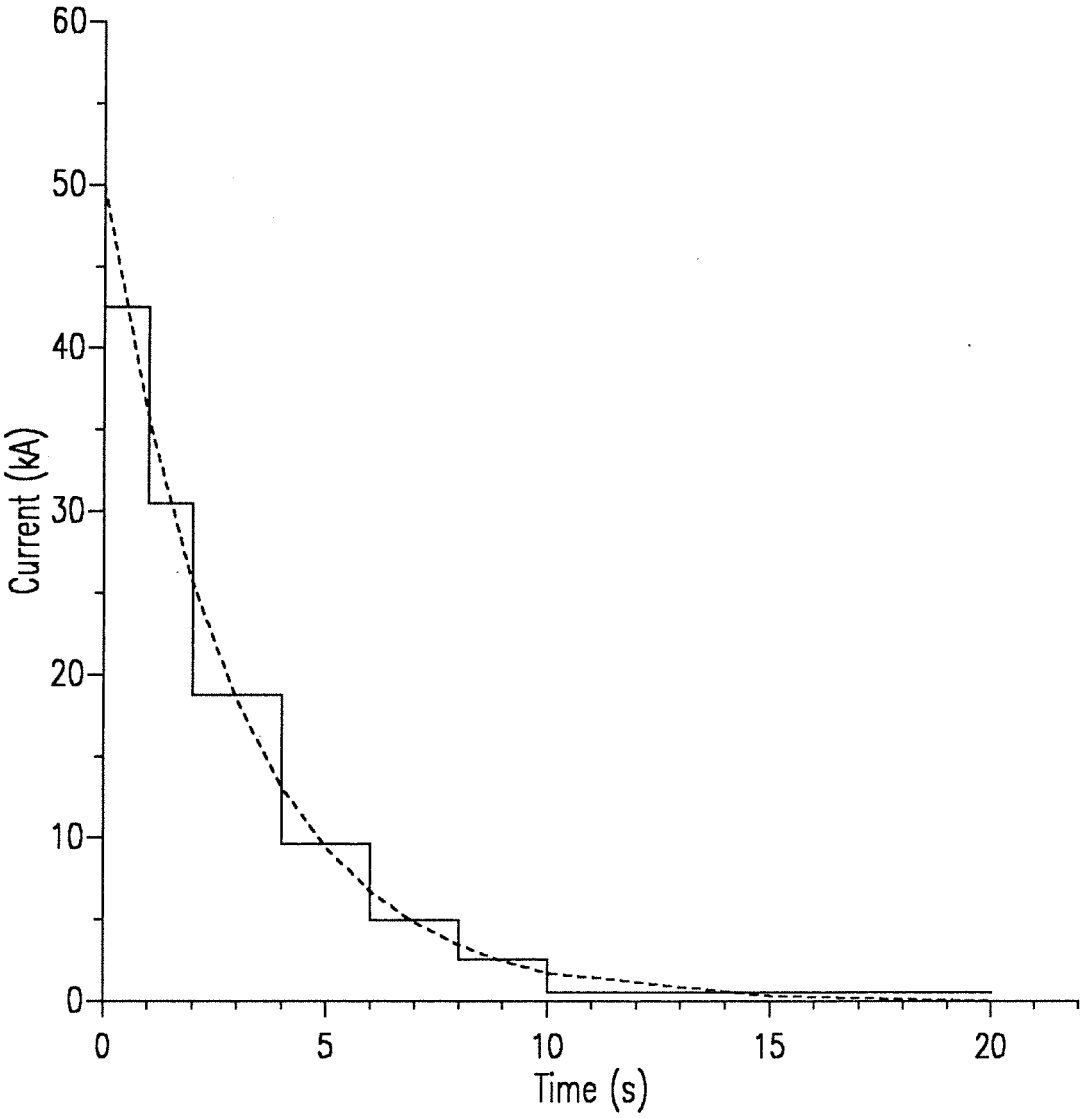


**Figure 16. Dump time vs time with $\tau$ = 3 s:** The dashed line denote the real dump current whereas the full line corresponds to the approximation used in the calculations

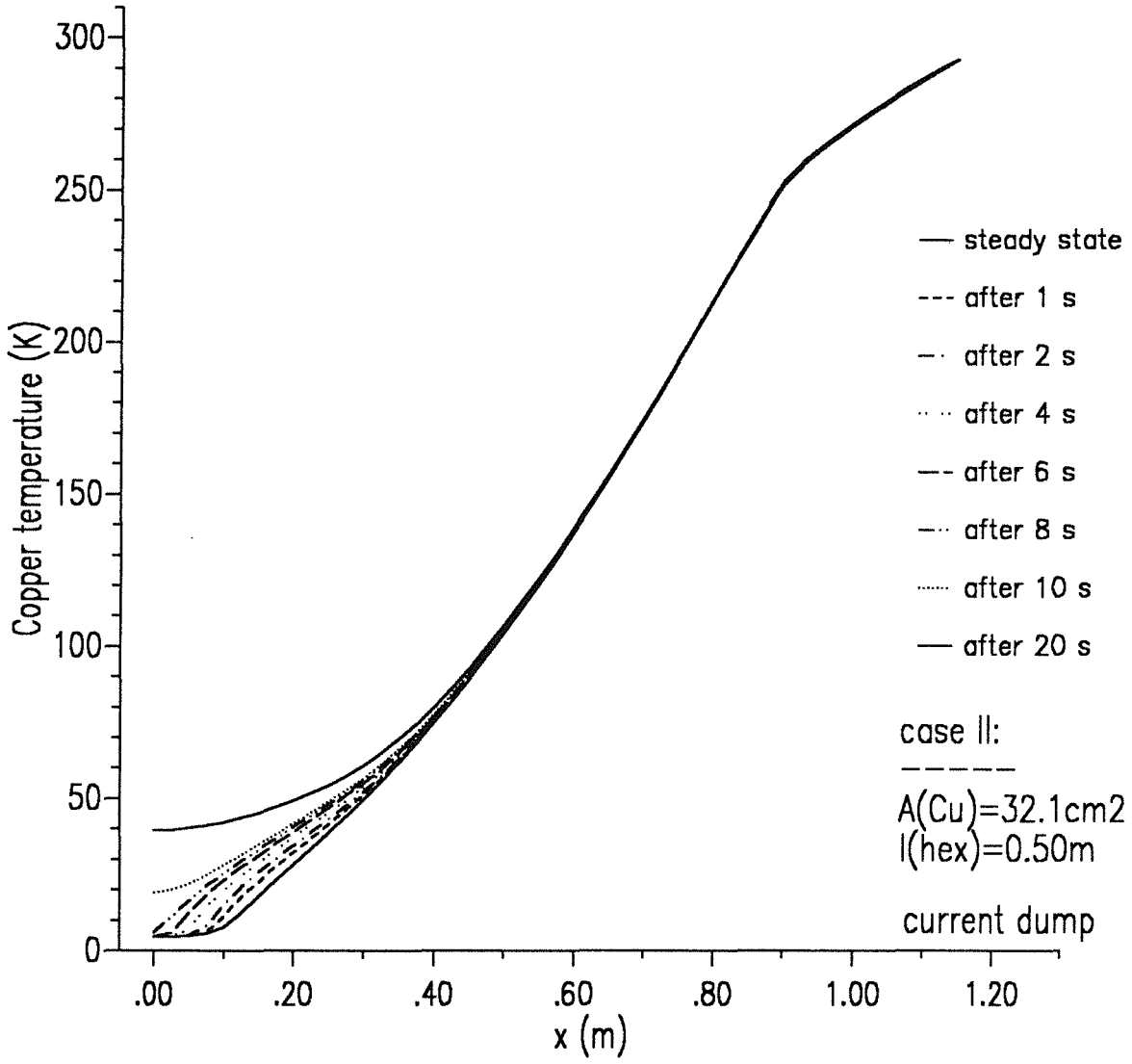


**Figure 17. Temperature distributions of the current lead in case of loss of mass flow and current dump with $\tau = 3$ s. The heat capacity of stagnant helium is considered (case I):** The different lines correspond to different times

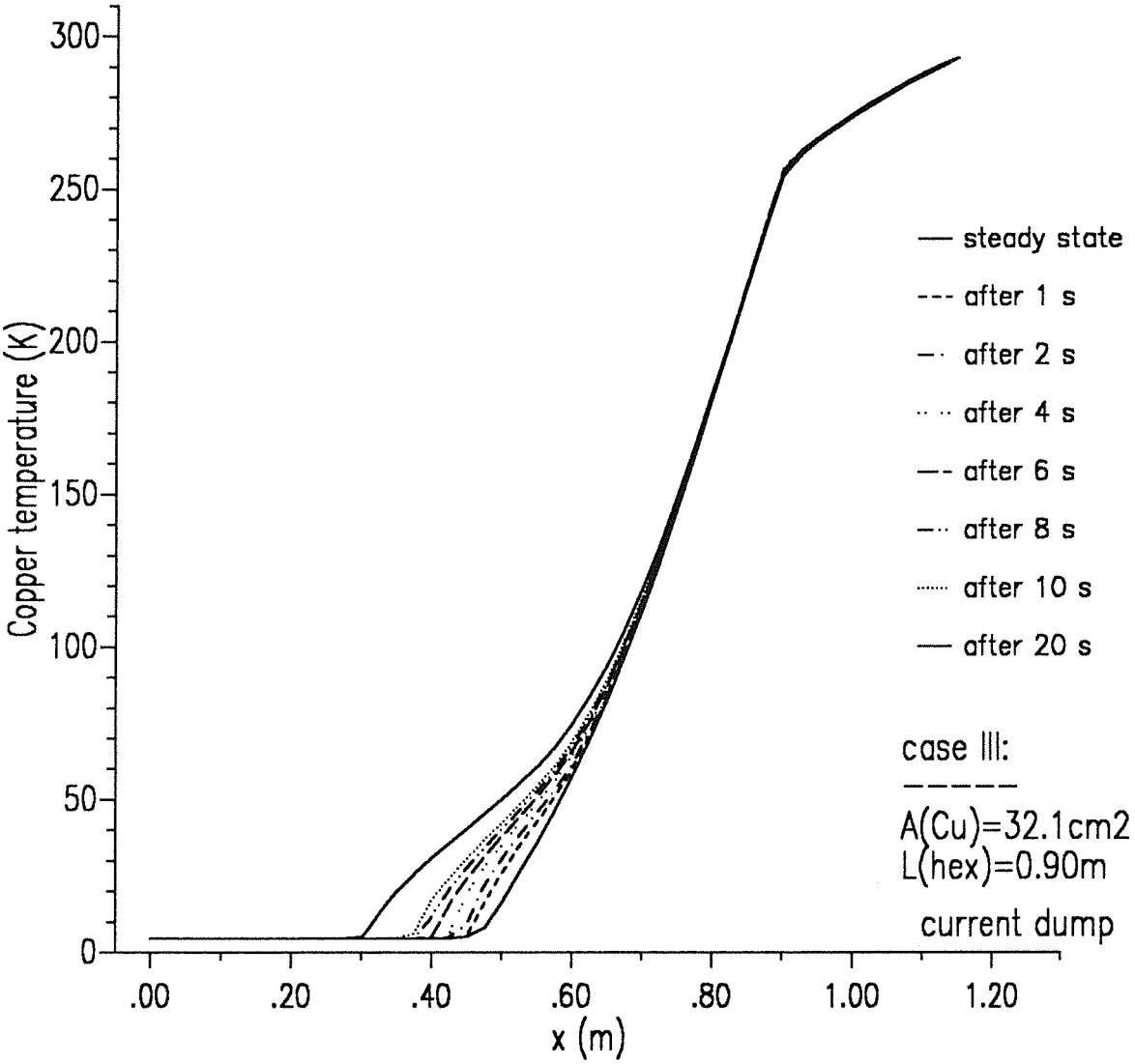


**Figure 18. Temperature distributions of the current lead in case of loss of mass flow and current dump with $\tau = 3$ s. The heat capacity of stagnant helium is considered (case III):** The different lines correspond to different times

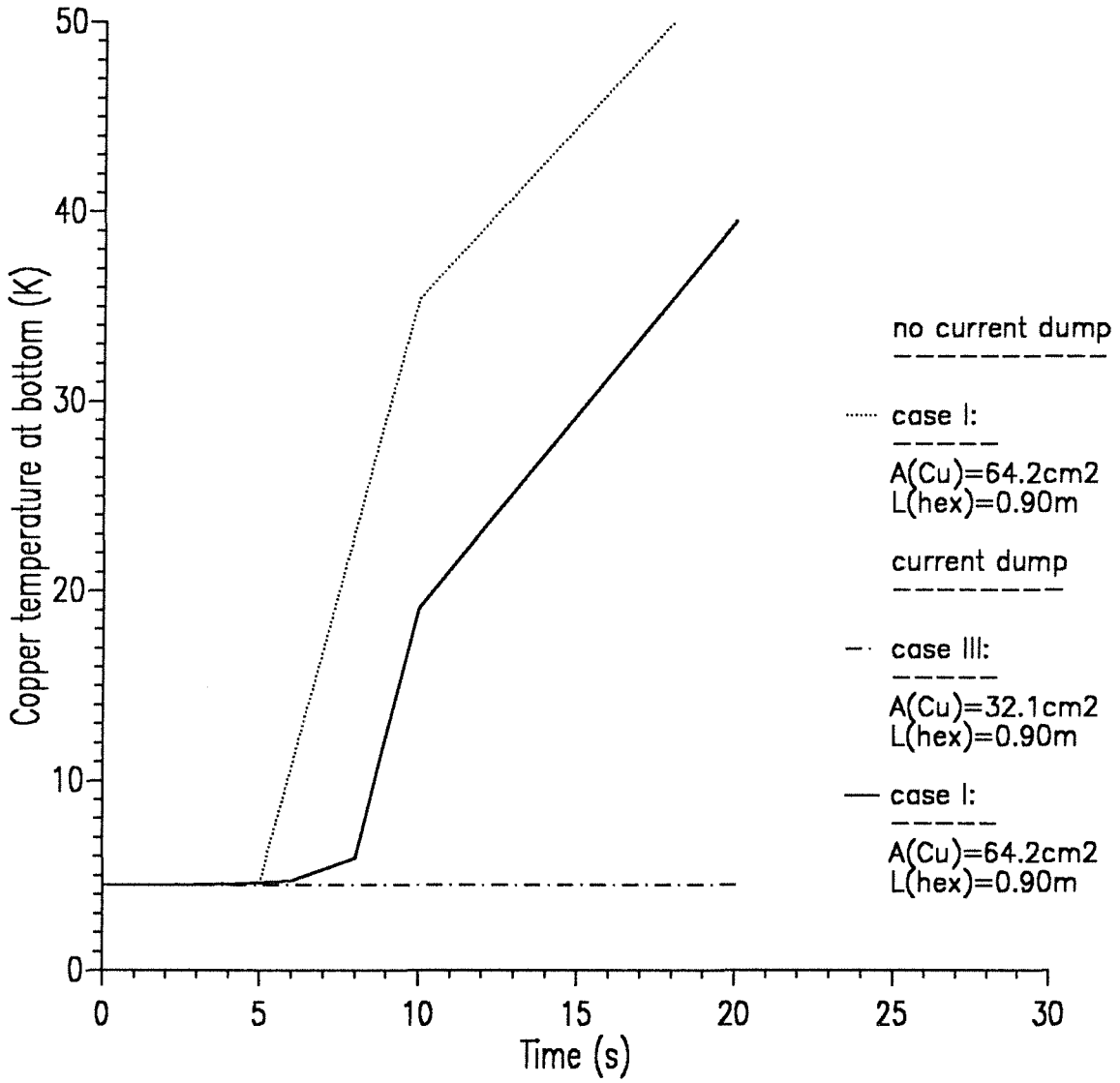


**Figure 19. Temperature of the conductor at the bottom end of the current lead vs time for 70 kA:** The dotted line represents the case I without current dump whereas the full resp. the dash-dotted line correspond to the case I resp. case II

| Time | $\dot{m}$ | ΔU | Δp | $T_{bottom}$ | $T_{cold}$ | $T_{max,Cu}$ | $T_{top,He}$ |
|---|---|---|---|---|---|---|---|
| [s] | $[\frac{g}{s}]$ | [mV] | [mbar] | [K] | [K] | [K] | [K] |
| case I<br>50 kA for 30 s without dump | | | | | | | |
| 1 | 0.0 | 72.6 | 0.0 | 4.51 | 23.2 | 293.0 | 293.0 |
| 5 | 0.0 | 74.9 | 0.0 | 4.63 | 35.0 | 293.0 | 293.0 |
| 10 | 0.0 | 76.6 | 0.0 | 35.43 | 44.3 | 293.0 | 293.0 |
| 20 | 0.0 | 79.0 | 0.0 | 53.63 | 55.8 | 293.0 | 293.0 |
| 30 | 0.0 | 80.1 | 0.0 | 58.67 | 61.0 | 293.0 | 293.0 |
| case I<br>50 kA for 30 s with current dump ($\tau = 3$ s) | | | | | | | |
| 1 | 0.0 | 61.6 | 0.0 | 4.51 | 22.7 | 293.0 | 293.0 |
| 2 | 0.0 | 44.5 | 0.0 | 4.52 | 25.6 | 293.0 | 293.0 |
| 4 | 0.0 | 27.6 | 0.0 | 4.56 | 29.0 | 293.0 | 293.0 |
| 6 | 0.0 | 14.3 | 0.0 | 4.69 | 31.3 | 293.0 | 293.0 |
| 8 | 0.0 | 7.4 | 0.0 | 5.91 | 33.2 | 293.0 | 293.0 |
| 10 | 0.0 | 3.9 | 0.0 | 19.09 | 34.9 | 293.0 | 293.0 |
| 20 | 0.0 | 0.8 | 0.0 | 39.52 | 45.3 | 293.0 | 293.0 |
| case III<br>50 kA for 30 s with current dump ($\tau = 3$ s) | | | | | | | |
| 1 | 0.0 | 65.7 | 0.0 | 4.50 | 42.7 | 293.0 | 293.0 |
| 2 | 0.0 | 47.7 | 0.0 | 4.50 | 45.7 | 293.0 | 293.0 |
| 4 | 0.0 | 29.9 | 0.0 | 4.50 | 48.8 | 293.0 | 293.0 |
| 6 | 0.0 | 15.6 | 0.0 | 4.50 | 50.9 | 293.0 | 293.0 |
| 8 | 0.0 | 8.1 | 0.0 | 4.50 | 52.7 | 293.0 | 293.0 |
| 10 | 0.0 | 4.2 | 0.0 | 4.50 | 54.3 | 293.0 | 293.0 |
| 20 | 0.0 | 0.9 | 0.0 | 4.50 | 60.5 | 293.0 | 293.0 |

**Table 7. Main results for 50 kA transient (loss of mass flow)**

## 4. Summary and conclusions

The conclusion of the calculations presented above is as follows:

- **case I**:
  The current lead requires at 50 kA a mass flow rate of 2.7 g/s. For a bath cooled current lead this would correspond to 1.13 W/kA. The helium consumption at zero current is about 50 percents of the one at nominal current. The latter one is not optimal but acceptable. The reason for the relatively high number lies in the fact that for acceptable conductor cross sections the length of the heat exchanger has to be relatively short (to be optimum for 50 kA and acceptable for 70 kA). The prize one has to pay for is a relatively high heat leak due to heat conduction which leads to a high helium consumption at zero current. Calculations with (slightly) different cross sections (and lengths) have shown that the change in the mass flow rate is only small.
  The temperature increase during the over-current within 30 s looks acceptable if taking into account the heat capacity of the helium at four bars.
  The temperature increase during the loss of coolant within 20 s while dumping the current is too high to let the superconducting bus superconducting. The conclusion is that an additional heat capacity is needed to store the energy.

  The only possibility to overcome the relatively high loss at zero current this is a drastic change in he geometry e.g. a factor of two in the conductor cross section therefore a factor of two in length.
- **case II**:
  The results are not quite different to the ones of case I i.e. no advantage at all.

  The third step was the increase of the length of the conductor in the heat exchanger equipped with $Nb_3Sn$ superconductors from 150 mm to 550 mm. The results are
- **case III**:
  The mass flow rate for the stand-by condition drops from 1.4 g/s to 0.75 g/s due the longer length of the conductor.
  The over-current scenario of 70 kA for 30 s as well as the fault conditions i.e. loss of mass flow throuh the current lead and a consecutive current dump with a time constant of $\tau = 3$ s lead to no increase of the bottom temperature. The heat capacity of the 550 mm long conductor equipped with superconductors is large enough to store the energy for a short time.

The conclusion is that the advantage of a high current density current lead is only true in combination of a long conductor part equipped with superconductor. This leads to a reduction in stand-by losses and an additional safety factor in case of a 70 kA over-current as well as in case of the loss of mass flow at 50 kA and a consecutive dump of the model coil. But the disadvantage is the fact that the lead looks more unstable if running near the minimum acceptable mass flow rate at high currents. This results in a slightly higher mass flow rate.

It should be noted that the computational results decribed in this report have to be verified by tests of the current leads built for the POLO model coil which will be done soon. This is important for

the confidence of these results because those current leads have been optimized by using the CURLEAD code.

The authors propose the current lead design case III i.e. the lead with the higher current density and the longer superconducting part of the heat exchanger which drastically reduces the bottom end heat losses. A schematic of the lead is shown in Figure 20 (not in scale) whereas the geometrical input data are given in Table 8.

| Parameter | Unit | Value |
|---|---|---|
| Overall length | m | 0.90 |
| Length of $Nb_3Sn$ wires | m | 0.55 |
| Cross section of conductor $A_{Cu}$ | $cm^2$ | 32.1 |
| Cooled perimeter of heat exchanger $P_{cool}$ | m | 8.85 |
| Cross section of helium $A_{He}$ | $cm^2$ | 30.05 |
| Inner diameter of cooling disks | cm | 6.5 |
| Outer diameter of cooling disks | cm | 13.57 |
| Transversal distance of cooling disks | mm | 2 |
| Disk thickness | mm | 1 |
| Hole diameter in cooling disks | mm | 1.6 |
| Minimum hole distance in cooling disks | mm | 2.5 |
| RRR of cooling disks | | 50 |
| Rib efficiency of cooling disks | | function of temperature |

**Table 8. Input parameters of the heat exchanger for the proposed current** lead (calculation case III)

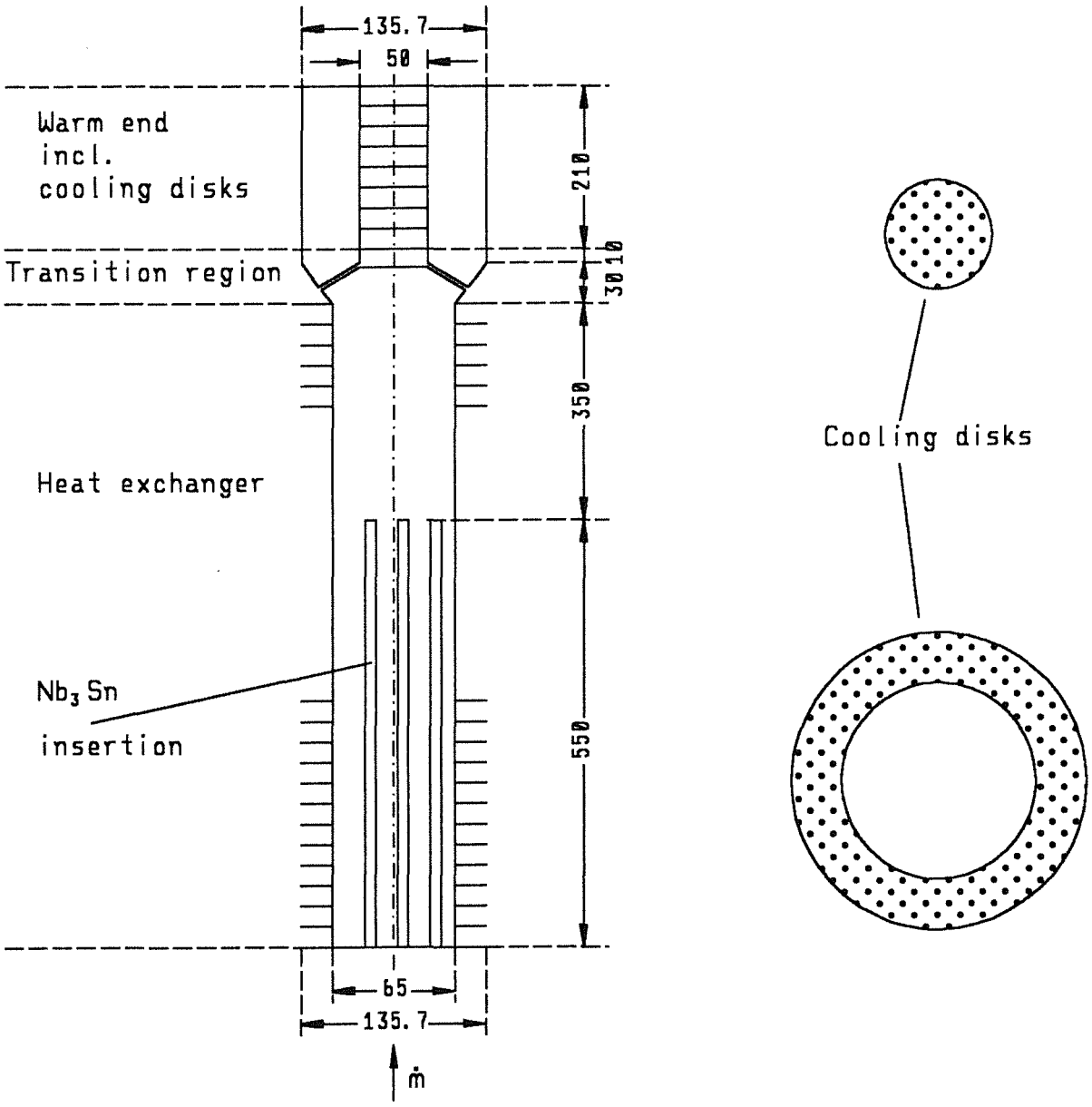


**Figure 20. Schematic of the current lead (case III)**

## Acknowledgement

This work has been performed within the frame of the European Fusion Technology Programme.

## 5. References


[1] R. Annandale, D. Besette, L. Bottura, P. Bruzzone, D. Ciazynski, H. Katheder, P. Libeyre, N. Mitchell, M. Perella, D. Robinson, E. Salpietro and B. Turck, "Concept Definition and Analysis of the NET Model Coils", NET report N/R/0221/1/E, 22.1.1991

[2] M.N. Wilson, "Superconducting Magnets", Clarendon Press, Oxford 1983

[3] R. Heller, "Numerical calculation of current leads for fusion magnets", KfK 4608, (1989)

[4] R. Heller and U. Jeske, unpublished report, Kernforschungszentrum Karlsruhe, 1989